iScience

CellPress
OPEN ACCESS

Article

Drosophila Aversive Behavior toward *Erwinia carotovora carotovora* Is Mediated by Bitter Neurons and Leukokinin

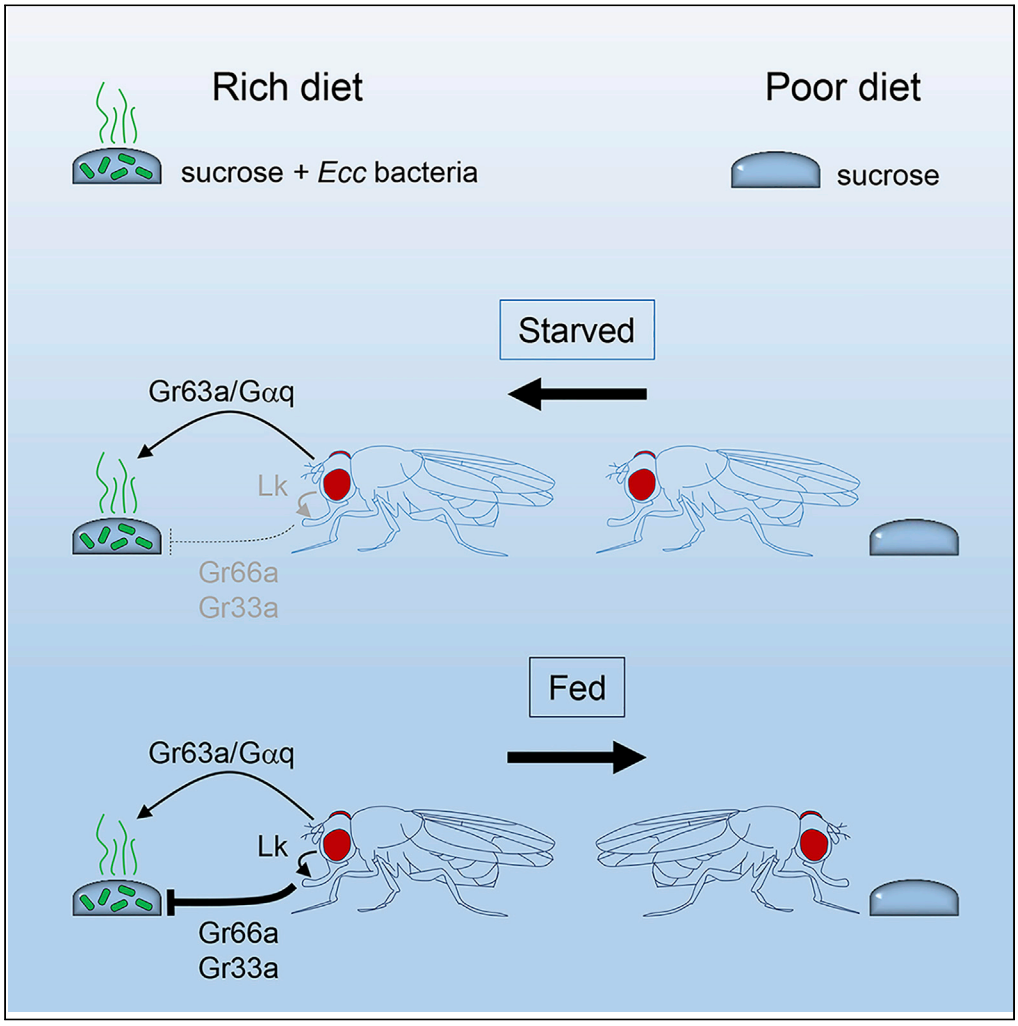

Bernard Charroux, Fabrice Daian, Julien Royet

bernard.charroux@univ-amu.fr (B.C.)
julien.royet@univ-amu.fr (J.R.)

HIGHLIGHTS

Starved flies are first attracted and then repulsed by *Erwinia*-contaminated solution

Flies' attraction to *Erwinia* is mediated by the olfactory receptor Gr63a and Gαq

Flies repulsion' to *Erwinia* requires Gr66a neurons and the leukokinin neuropeptide

Feeding on *Erwinia*-contaminated solution potentiates bitter neurons of starved flies

Charroux et al., iScience *23*, 101152
June 26, 2020
https://doi.org/10.1016/j.isci.2020.101152

iScience

CellPress
OPEN ACCESS

Article

Drosophila Aversive Behavior toward *Erwinia carotovora carotovora* Is Mediated by Bitter Neurons and Leukokinin

Bernard Charroux,[1,*] Fabrice Daian,[1] and Julien Royet[1,2,*]

SUMMARY

The phytopathogen *Erwinia carotovora carotovora* (*Ecc*) has been used successfully to decipher some of the mechanisms that regulate the interactions between *Drosophila melanogaster* and bacteria, mostly following forced association between the two species. How do *Drosophila* normally perceive and respond to the presence of *Ecc* is unknown. Using a fly feeding two-choice assay and video tracking, we show that *Drosophila* are first attracted but then repulsed by an *Ecc*-contaminated solution. The initial attractive phase is dependent on the olfactory Gr63a and Gαq proteins, whereas the second repulsive phase requires a functional gustatory system. Genetic manipulations and calcium imaging indicate that bitter neurons and gustatory receptors Gr66a and Gr33a are needed for the aversive phase and that the neuropeptide leukokinin is also involved. We also demonstrate that these behaviors are independent of the NF-κB cascade that controls some of the immune, metabolic, and behavioral responses to bacteria.

INTRODUCTION

In nature, animals, including insects, thrive in an environment with constant exposure to microorganisms. Over the evolution times, insects have established various types of associations with microorganisms that may be classified as mutualistic, commensalistic, saprophytic, or parasitic (Douglas, 2014). Besides, some insects are major vectors of plant and animal diseases, spreading microorganisms throughout animal and plant kingdoms. In all these cases, insects must sample their contaminated environment to identify the type of microorganisms in which they are in contact and to engage in adapted behaviors. As for other biological processes that need to be molecularly characterized, identification of the players and the mechanisms that insects use to perceive microorganisms and to react adequately is greatly facilitated by the use of model organisms. Over the last 30 years, *Drosophila* has emerged as a very powerful model for modeling the interactions between bacteria and insects (Buchon et al., 2014) (Bergman et al., 2017; Capo et al., 2016; Lee and Lee, 2014; Lestradet et al., 2014). These studies, which allowed the discovery of fundamental immune mechanisms regulating invertebrate-bacteria interactions, relied on a relatively small number of bacteria species, including *Escherichia coli* (*E. coli*), *Pseudomonas entomophila*, *Serratia marcescens*, and *Erwinia carotovora carotovora* (*Ecc*) (Acosta Muniz et al., 2007; Basset et al., 2000; Bosco-Drayon et al., 2012; Buchon et al., 2009; Haller et al., 2014; Nehme et al., 2007; Quevillon-Cheruel et al., 2009; Royet et al., 2011; Vodovar et al., 2005). The present study focuses on one of them, *Ecc* also named *Pectinobacterium carotovorum*. Naturally transmitted by insects, this phytopathogenic organism that causes soft rot in fruits has been intensively used to decipher the mechanisms that control host-pathogen interactions in the *Drosophila* model (Buchon et al., 2014). When used to orally infect *Drosophila* larvae or adults, *Ecc* is not only able to trigger a local immune response in the gut epithelium but also a systemic activation of one the NF-κB signaling cascade, named IMD, in immunocompetent organs bathing in the hemolymph (Basset et al., 2000; Vodovar et al., 2005). This characteristic, which reflects the ability of gut-born *Ecc*-derived peptidoglycan to cross the gut epithelium and reach the hemolymph, has been used to study the impact that gut microbiota can exert on the host (Charroux et al., 2018; Kurz et al., 2017). Indeed, detection of gut-derived PeptidoGlycaN (PGN) by receptors belonging to the peptidoglycan recognition protein family (PGRP) has a very strong influence on many aspects of host metabolism and also on fly behavior (Royet et al., 2011). However, in all previous studies, wherein the impact of *Ecc* on *Drosophila* larvae or adult has been tested, animals are orally infected following forced oral association with *Ecc* for few to many hours. This protocol, which is non-natural, could induce biases in the interpretation of the obtained results.

[1]Aix-Marseille Université, CNRS, IBDM, Marseille, France

[2]Lead Contact

*Correspondence: bernard.charroux@univ-amu.fr (B.C.), julien.royet@univ-amu.fr (J.R.)

https://doi.org/10.1016/j.isci.2020.101152

We therefore decided to analyze the behavior of *D. melanogaster* adults confronted with food sources contaminated by *Ecc*. To do so, we developed a two-choice feeding assay where flies have the possibility to feed either on an axenic solution or on *Ecc*-contaminated media. Using time-lapse video recording, we show that *D. melanogaster* adult flies display a robust stereotyped behavior. They are first attracted by the bacterial solution that they ingest, before showing, after a long period only, a strong aversion toward *Ecc* and deciding to move away to feed on the axenic solution. Our results show that if olfactory cues and, more specifically, the Gr63a receptor participate in the initial attraction phase, the subsequent aversion phase relies on gustatory neurons expressing Gr66a receptors. We also show that aversion to *Ecc* requires the Gr66a and Gr33a bitter receptors as well as the neuropeptide leukokinin (Lk) but does not involve the chemosensory cation channel and lipopolysaccharide (LPS) receptor TrpA1 or the IMD innate immune pathway.

RESULTS

Using Time-Lapse Video Recording to Study Fly Feeding Choice

To investigate the impact that a contamination by *Ecc* has on adult fly feeding behavior, we developed an experimental setup to video record flies' movements during a two-choice feeding experiment. This apparatus can record in live the feeding behavior of multiple flies in arenas simultaneously (See Methods). Experiments were performed with 10 or 20 females per arena that were starved overnight. Before adding flies into the arenas, two drops of feeding solution were positioned at a precise distance from each side of the arena (Figure 1A). To track flies' movements, we mounted a webcam on top of the multi-arena apparatus. One image was acquired every 5 s during a period of 6 h, and the movies were created by combining 10 images per second.

We started with the assumption that flies attracted by a feeding solution should spend more time close to it than to the other solution. Such a behavior was observed when flies were given the choice between a drop of 50 mM sucrose and a drop of water (Figure 1A and Video S1). Most of the time (from roughly t = 1 h until t = 6 h), the flies stayed in close vicinity to the sucrose solution. As a consequence of fly feeding, the size of the drop progressively diminished (Video S1). We analyzed and quantified this behavior over time by calculating an attraction index (AI) for each time frame as follows. The distance of each of the 10 females from droplet 1 (d1) and droplet 2 (d2) was measured every 5 s, and the AI was calculated as the log_2 ratio of the average of distances d1 divided by the average of distances d2. The d2 attraction will be translated into a positive index, and the d1, by a negative one. We then calculated a cumulative AI (CAI) corresponding to the area between the AI curve and the abscissa axis for x = 0, which represents the absolute preference of the flies for each of the two feeding solutions. We then could calculate the preference index (PI) for the solution 1 as follows: PI (solution 1) = (CAI solution 1)-(CAI solution 2)/(CAI solution 1)+(CAI solution 2). An example of such an analysis is shown in Figures 1A–1C, where flies were given the choice between water (solution 1) and a 50 mM sucrose solution (solution 2). The AI calculated for eight experimental replicates showed that during the first 45 min, flies were not preferentially positioned close to any of the two solutions. From then on, the flies got closer to the sucrose solution until the end of the movie (Video S1). Hence, once the choice has been made, it stayed robust and was not alterable over time. The CAI for sucrose (>4,000 a.u.) and the PI for sucrose of 0.97 indicated that flies had a clear preference for sucrose over water, as we could have expected for a gustatory attractive substance. Note that during the 6 h movie, we observed a reduction in the size of the feeding solution drop chosen by the flies as well as a progressive appearance of small deposits around the flies corresponding very likely to feces (Video S1).

We then tested our device with flies that were given the choice between sucrose solutions, one at 5 mM and the other at 50 mM (Figures 1B and 1C). The AI curve displayed in Figure 1B showed that flies were more attracted by the highly concentrated sucrose solution. No obvious choice was made when the flies were given the choice between two equimolar sucrose solutions (Figures 1A and 1B). When the flies were given the choice between a sweet (50 mM sucrose) and a bitter solution (50 mM sucrose +10 mM caffeine) (Video S1) the aversion of the bitter solution started less than 30 min after the beginning of the experiment and lasted for the next five and a half hours. Once again, flies made a robust and permanent choice to avoid caffeine with a CAI for sucrose over 4,500 a.u. and a PI for caffeine of −0.98 (Figures 1B and 1C).

D. melanogaster Are First Attracted by *Ecc* but Then Repulsed by It

We next explored the behavior of adult females in the presence of two feeding solutions, one containing *Ecc* bacteria in 50 mM sucrose and the other 50 mM sucrose only. Collected data revealed that flies

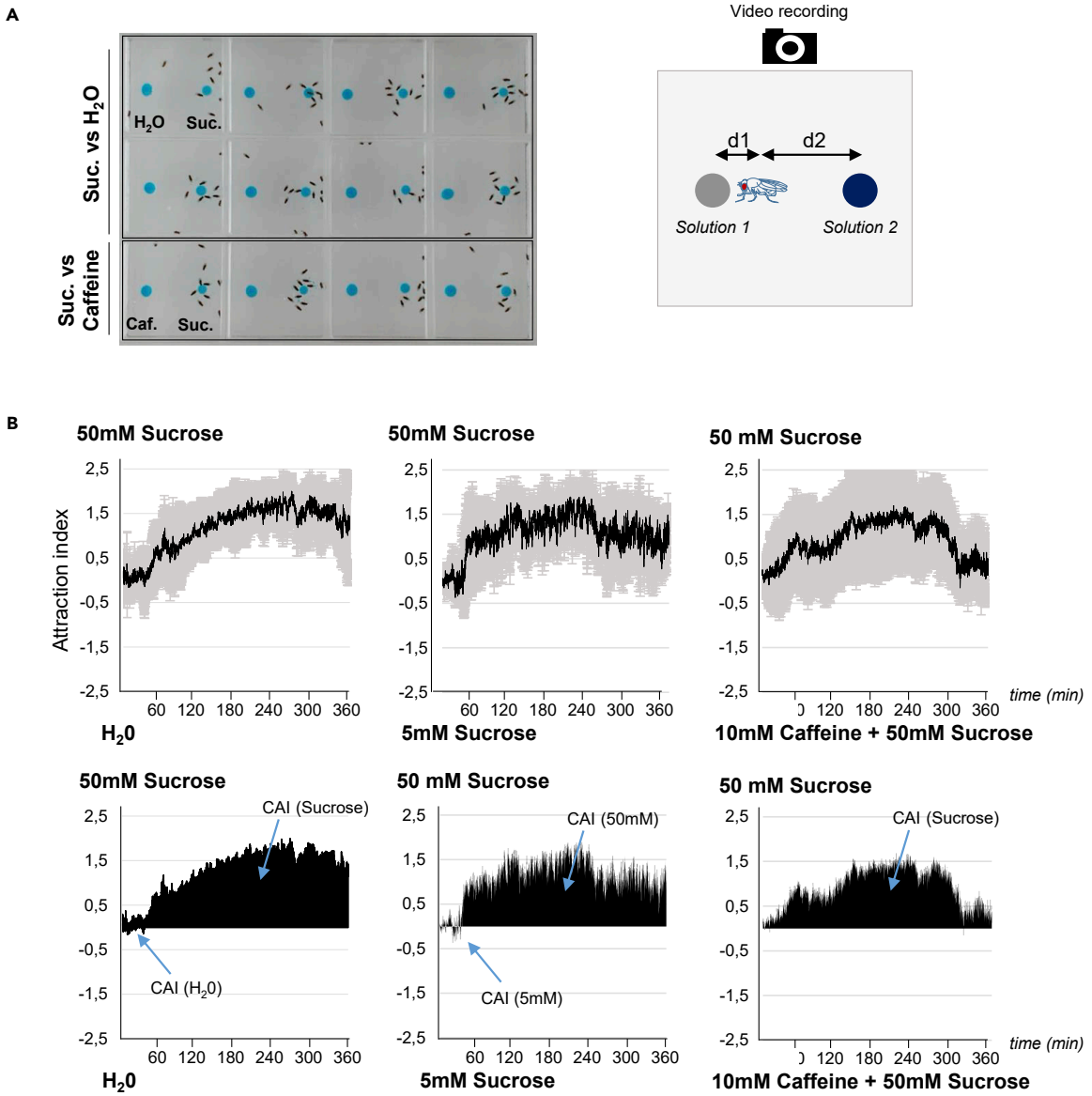
A
Suc. vs H2O
H2O
Suc.
Suc. vs Caffeine
Caf.
Suc.
Video recording
d1
d2
Solution 1
Solution 2
B
50mM Sucrose
H2O
50mM Sucrose
5mM Sucrose
50 mM Sucrose
10mM Caffeine + 50mM Sucrose
Attraction index
time (min)
50mM Sucrose
CAI (Sucrose)
CAI (H20)
H2O
50 mM Sucrose
CAI (50mM)
CAI (5mM)
5mM Sucrose
50 mM Sucrose
CAI (Sucrose)
10mM Caffeine + 50mM Sucrose
C
Cumulative AI for 6h (a.u)
n=8
H2O
Sucrose
n=6
5mM Sucrose
50mM Sucrose
n=12
Caffeine + Sucrose
Sucrose
Preference index
Sucrose (H20 vs Sucrose)
Caffeine
50mM Sucrose (5mM vs 50mM)

Figure 1. *Drosophila* Females Were Attracted by Sucrose and Avoid Caffeine

(A) (Left) Still frame taken during the video recording (t = 240 min) of an experiment with 12 arenas, each containing 10 females and two drops of feeding solution (in blue). The top 8 arenas contain one drop of H_2O (left) and one drop of 50 mM sucrose (right). The bottom 4 arenas contain one drop of 50 mM sucrose + 10 mM caffeine (left) and one drop of 50 mM sucrose (right). (Right) The drawing illustrates the 2 distances (d1 and d2) measured at every time frame of the video (see main text).

(B) Flies displayed a strong preference for sucrose and aversion to caffeine + sucrose. (Top) Per graphs: Kinetics of the attraction index (AI) for sucrose in a sucrose versus H_2O experiment (left), in a 50 mM sucrose versus 5 mM sucrose experiment (middle), or in a sucrose versus sucrose + caffeine experiment (right). The black lines and the gray zones correspond, respectively, to the mean and the standard deviation. (Bottom) Cumulative attraction index (CAI) area for each specified solution (arrows) and its distribution over time. For simplicity, only the mean value of the CAI obtained with multiple replicates is shown in black.

(C) Histograms built with the CAI values from (B) showing that flies have a strong and statistically significant preference for sucrose versus H_2O and for 50 mM sucrose versus 5 mM sucrose and a strong aversion for a mixture of caffeine + sucrose versus sucrose only. *$p < 0.05$ and **$p < 0.01$. Wilcoxon matched-pairs signed rank test, Two-tailed p value. Error bars correspond to standard deviation. The preference indexes for sucrose, for 50 mM sucrose, and for caffeine are calculated with the CAI values from C. n indicates the number of independent experimental replicates. a.u.: arbitrary unit. Data are represented as mean ± SD.

displayed a two-step stereotyped behavior. They were first attracted by the contaminated solution before moving away from it and staying close to the sucrose solution permanently (Video S2). The CAI for *Ecc* was lower (552 a.u. +/− 381 SD) than for sucrose (3,918 a.u. +/− 1291 SD), and the preference index for *Ecc* was negative (−0.72 ± 0.2 SEM) (Figures 2A and 2B). This indicated that flies displayed a global aversion toward *Ecc*. However, the video tracking helpfully revealed the presence of two distinct phases throughout the experiment. Flies were first attracted by the *Ecc* solution (for approximately 60 min), whereas they were later preferentially found in the proximity to the sucrose solution. Identical results were obtained when positions of sucrose and *Ecc* solutions were randomized showing that there was no directional bias (Figures S1C and S1D). A similar biphasic curve was obtained using males, indicative of an absence of sex-biased comportment of *D.* melanogaster toward *Ecc* (Figures 1E and 1F).

Flies' Attraction to *Ecc* Is Mediated by the *Gr63a* and *Gαq*

We then tested which of the sensory system(s) controls the initial attractive phase. As flies were first attracted by bacteria, we tested whether the gustatory sweet pathway, known to be involved in fly's attractiveness, was involved. For this purpose we took advantage of a "sugar-blind" strain in which all nine sugar gustatory receptor genes are deleted (Yavuz et al., 2014). *R1Gr5a^{LexA}; Gr43a^{-}; ΔGr61a,ΔGr64a-f* flies showed the same behavior as control flies demonstrating that the sweet pathway is not involved in the initial attraction phase to *Ecc* (Figures 2D and 2E). This result was confirmed using Gr5a-Gal4; UAS-Kir2.1 flies in which the sweet neurons are inactivated (Figures 2F and 2G). From previous studies, we hypothesized that flies could be attracted by the odors emanating from the bacterial solution (Kapsetaki et al., 2014; Stensmyr et al., 2012). To test this hypothesis, we analyzed the contributions of members of the odorant receptor (Or) gene family using flies lacking the obligate Or co-receptor Orco. *Orco* mutant flies behaved as wild-type controls when given the choice between sucrose and *Ecc* solutions (Figures S2A and S2B). We finally tested the putative implication of an inhibition of the CO_2-sensing neurons in the attraction phase. Previous work has indeed shown that *D. melanogaster* can sense CO_2 via a heterodimeric receptor composed of two members of the gustatory receptor family Gr21a and Gr63a (Jones et al., 2007; Kwon et al., 2007). Although CO_2 is normally repulsive to adult flies, compounds such as polyamines are attractive by antagonizing this Gr63a/Gr21a-dependent CO_2 repulsion (MacWilliam et al., 2018; Turner and Ray, 2009). The attractiveness of polyamines such as spermidine is therefore lost in Gr63a or Gr21a mutants. We found that whereas heterozygous Gr63a mutants behaved as wild-type flies, Gr63a homozygous mutants were no longer attracted by *Ecc* (Figures 3A and 3B). Interestingly, this lack of attractiveness for *Ecc* was associated with a delay in the establishment of the repulsive phase (see later). Similar phenotypes, including a loss of the initial attraction and a delay of the subsequent repulsion, were observed using mutants for the G protein (Gαq) that transduces the GR63a/Gr21a receptor signal (Figures 3C and 3D) (Yao and Carlson, 2010). These results demonstrate that the attraction of flies toward *Ecc* is independent of the sweet gustatory pathway and of the Orco-mediated olfactory pathways but requires GR63a and Gαq. It remains to be demonstrated whether Gr63a and Gαq are acting in the same cells and therefore in a linear pathway.

Ecc Aversion Is Not due to Medium Modification

As the repulsive phase required a long time to be established, we wondered whether flies have ingested the bacteria-containing solution during the initial phase, before aversion is established. To address this question, we performed a two-choice feeding assay using *Ecc-GFP* fluorescent bacteria. After 90 minutes of having been deposited into the arenas, all the flies displayed a fluorescent crop, demonstrating they had

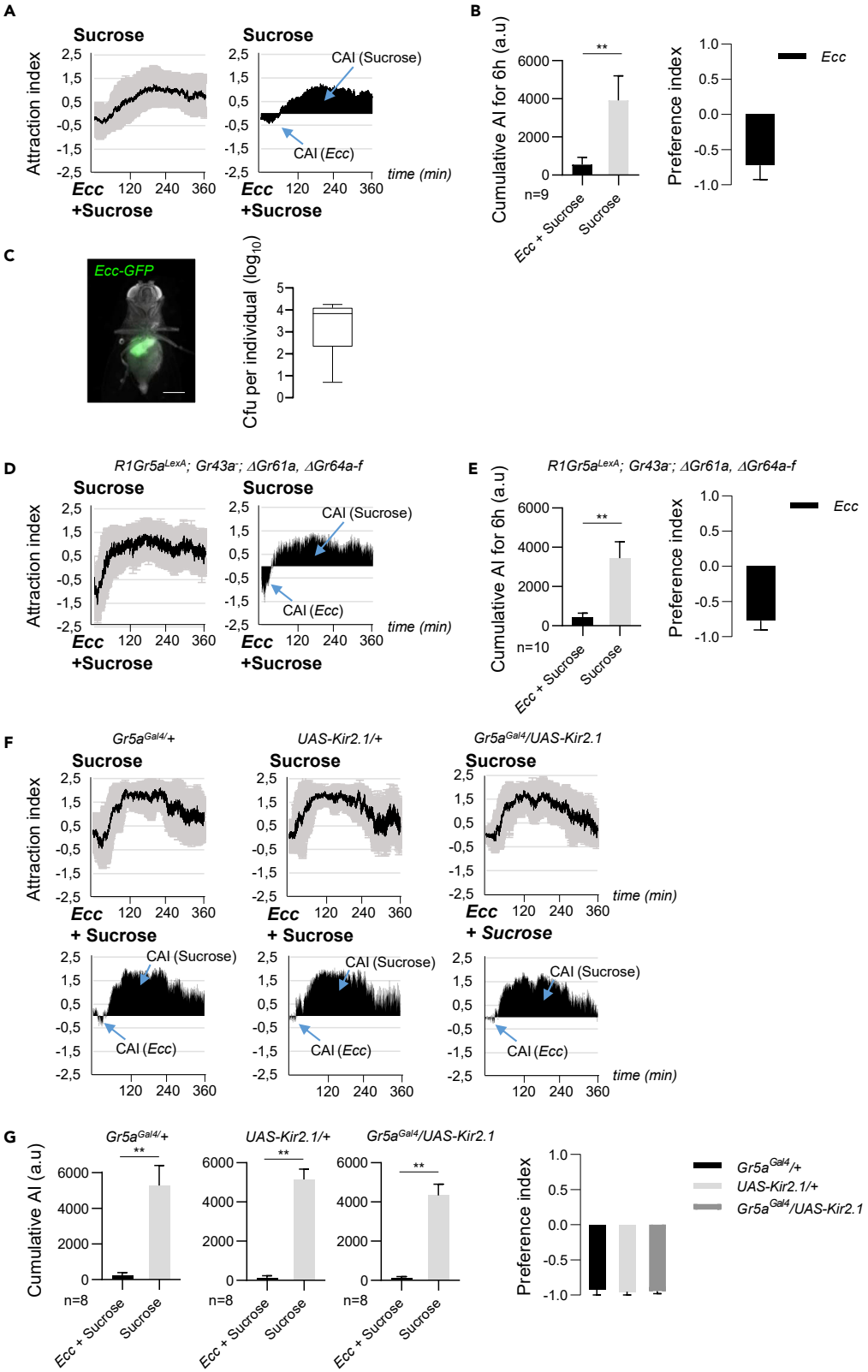
A
Sucrose
Attraction index
Ecc
+Sucrose
CAI (Sucrose)
CAI (Ecc)
time (min)
B
Cumulative AI for 6h (a.u)
n=9
Ecc + Sucrose
Sucrose
Preference index
Ecc
C
Ecc-GFP
Cfu per individual (log10)
D
R1Gr5aLexA; Gr43a-; ΔGr61a, ΔGr64a-f
E
n=10
F
Gr5aGal4/+
UAS-Kir2.1/+
Gr5aGal4/UAS-Kir2.1
+ Sucrose
G
n=8

Figure 2. *D. melanogaster* Adults Were First Attracted by *Ecc* before Being Repelled by It

(A and B) Adult females displayed a two-step behavior when given the choice between an *Ecc*-contaminated sucrose solution and a sucrose-only solution. (A) (Left) Kinetics of the AI for sucrose in a sucrose versus sucrose + *Ecc* experiment. (Right) CAI area for each specified solution (arrows) and its distribution over time. (B) (Left) histograms built with the CAI values from A. **p value < 0.01. Wilcoxon matched-pairs signed rank test, two-tailed p value. Error bars correspond to standard deviation. The preference index for *Ecc* is calculated with the CAI values from (B).

(C) Flies ingested bacteria during the initial phase. Picture: ventral view of an adult female sampled at t = 90 min and showing *Ecc-GFP* bacteria accumulating in the digestive tract. Scale bar, 0.5 mm. Graph: Boxplot of colony-forming unit (CFU) analysis of individual flies sampled at t = 90 min.

(D and E) Sugar-blind flies of the *R1Gr5a^{Lexa}; Gr43a^{-}; ΔGr61a, ΔGr64a-f* genotype displayed a two-step behavior. (D) (Left) Kinetics of the AI for sucrose in a sucrose versus sucrose + *Ecc* experiment. (Right) CAI area for each specified solution (arrows) and its distribution over time.

(E) Histograms built with the CAI values from (D). **p value < 0.01. Wilcoxon matched-pairs signed rank test, Two-tailed p value. Error bars correspond to standard deviation. The preference index for *Ecc* is calculated with the CAI values from (D).

(F and G) Adult females expressing *UAS-Kir2.1* in sweet neurons using *Gr5a^{Gal4}* displayed aversion to *Ecc*. (F) (Top) Kinetics of the AI for sucrose. (Bottom) CAI area for each specified solution (arrows) and its distribution over time. (G) Histograms built with the CAI values from (F). **p value < 0.01. Wilcoxon matched-pairs signed rank test, Two-tailed p value. Error bars correspond to standard deviation. The preference indexes for *Ecc* are calculated with the CAI from (F).

For (A and D) left graphs and (F) top graphs, the black lines and the gray lines correspond, respectively, to the mean and the standard deviation, and for right graphs in (A and D) and bottom graphs in (F), solely the mean value of the CAI obtained with multiple replicates is shown in black. n indicates the number of experimental replicates. a.u.: arbitrary unit. Data are represented as mean ± SD.

indeed ingested bacteria (Figure 2C). When the same flies were plated for colony-forming unit (CFU) quantification, we found that all flies have eaten live bacteria (6.9×10^8 CFU/fly on average). In conclusion, *Ecc* ingestion preceded the fly's choice to move away and feed onto the bacterial free sucrose solution.

As aversion to *Ecc* is taking place after a 60- to 90-min latency period, we asked whether *Ecc* could metabolize the attractive sucrose solution and transform it into an aversive one via, for example, the release of aversive metabolic by-products. To test this hypothesis, we measured the attraction of *Ecc* bacteria pre-incubated 2 h with sucrose before being deposited into the arena. If indeed an incubation period of *Ecc* with sucrose was required to transform it from an attractant to an aversive solution, one might expect the pre-incubated solution to be aversive immediately without any latency. The attractive phase was not only still present when flies were put in the presence of a pre-incubated medium but also lasted longer than with the non-pre-incubated solution (Figures S2C and 2D). The aversion was therefore neither due to an *Ecc*-mediated sucrose modification nor due to an alteration of *Ecc* when put in the presence of sucrose.

D. melanogaster Behavior toward *Ecc* Is Independent of the IMD/NF-κB Pathway and LPS

In *D. melanogaster*, DiaminoPimelic Acid (DAP)-type peptidoglycan containing bacteria, such as *Ecc*, are sensed by pattern recognition receptors belonging to the PGRP family (Royet et al., 2011). Direct recognition of bacterial cell wall-derived PGN by either membrane-associated (PGRP-LC) or cytosolic (PGRP-LE) proteins activates the IMD signaling pathway (Charroux et al., 2018). This leads to the nuclear translocation of the NF-κB transcription factor Relish, a step required for the transcriptional activation of a set of immune effectors and regulators (Kleino and Silverman, 2014). For some bacteria such as *Ecc*, gut-born peptidoglycan can cross the gut epithelium and reach the circulating hemolymph where it gets in contact with remote tissues and organs in which it activates immune signaling (Basset et al., 2000; Bosco-Drayon et al., 2012). As bacteria can be found in the gut lumen within 1 h of the experiment, and because PGN can affect host signaling in a short period, we asked whether internal sensing of PGN was a required step to mediate the delayed aversive behavior.

We addressed this issue in two ways. First, we performed an experiment using heat-killed *Ecc* bacteria that no longer activated the gut local and the fat body systemic NF-κB responses (Basset et al., 2000 and Figure 4C). Although flies remained attracted to heat-killed bacteria, they no longer escaped from them and even fed on them during the 6 h that the experiment lasted (Figures 4A and 4B). This result indicated that either the IMD pathway activation is required to establish the aversive behavior, but not the attraction, and/or that the putative bitter substance(s) produced by *Ecc* is (are) heat sensitive. To directly test the implication of the NF-κB activation in establishing the aversion toward *Ecc*, we performed the experiment using live *Ecc* and flies null mutant for the Relish transactivator. The results indicated that

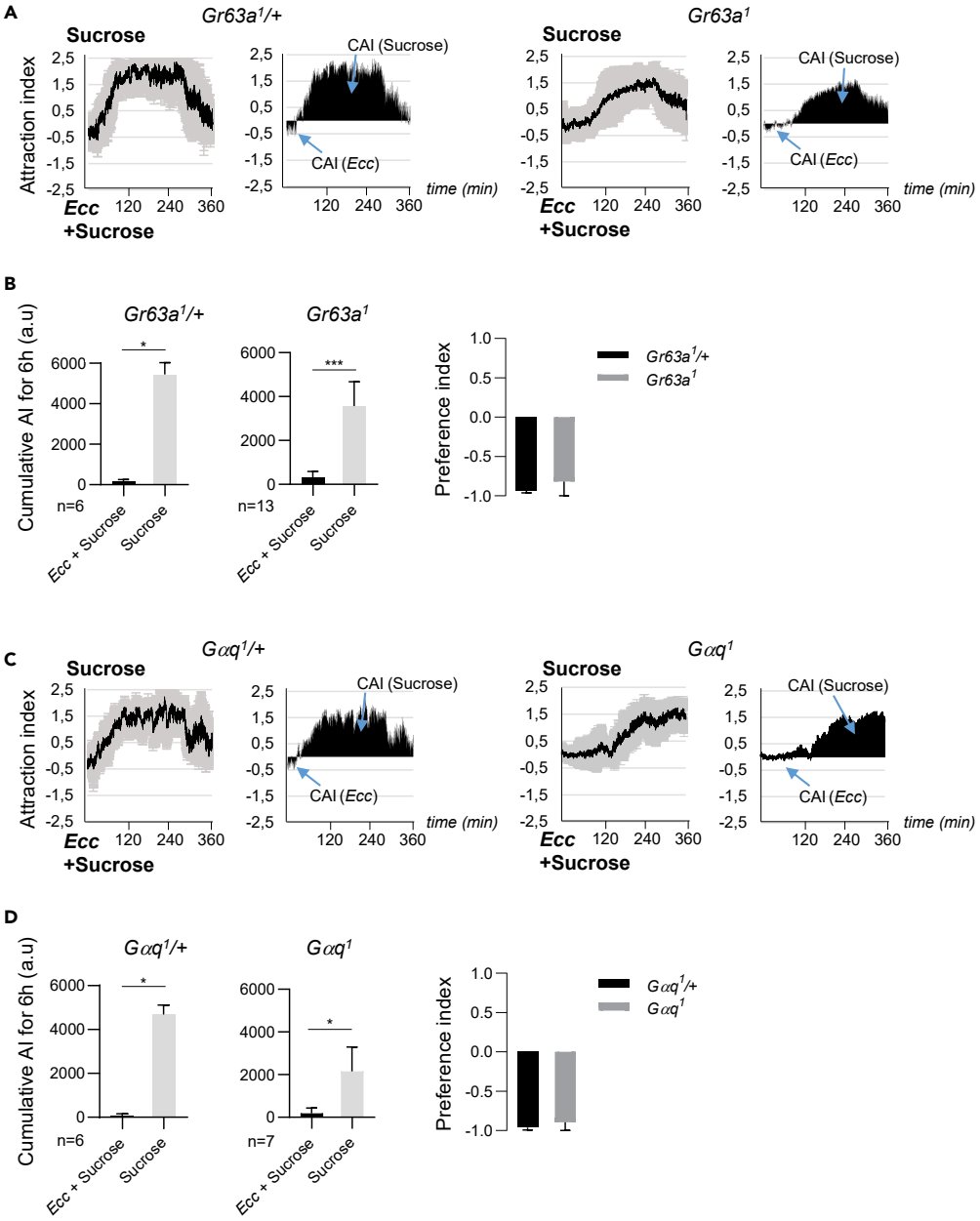

Figure 3. Flies Attraction to *Ecc* Is Mediated by *Gr63a and Gαq*

(A and B) Flies homozygous for the loss-of-function allele *Gr63a*^{1} displayed no attraction to *Ecc*, and a delayed aversion to the bacteria, whereas control *Gr63a*^{1}/+ behaved normally. (A) (Left graphs) Kinetics of the AI for sucrose. (Right graphs) CAI area for each specified solution (arrows) and its distribution over time. (B) Histograms built with the CAI values from (D). *p < 0.05 and ***p < 0.001. Wilcoxon matched-pairs signed rank test, two-tailed p value. Error bars correspond to standard deviation. The preference indexes for *Ecc* are calculated with the CAI values from (B).

(C and D) Flies homozygous for the hypomorphic allele *Gαq*^{1} displayed reduced attraction to *Ecc*, whereas control *Gαq*^{1}/+ showed a usual one. (C) (Left) Kinetics of the AI for sucrose. (Right) CAI area for each specified solution (arrows) and its distribution over time. (D) (Right) Histograms built with the CAI values from (D). *p < 0.05. Wilcoxon matched-pairs signed rank test, two-tailed p value. Error bars correspond to standard deviation. The preference indexes for *Ecc* are calculated with the CAI values from (D). For (A and C) (left graphs) the black lines and the gray lines correspond, respectively, to the mean and the standard deviation, and (right graphs) solely the mean value of the CAI obtained with multiple replicates is shown in black. n indicates the number of experimental replicates. a.u.: arbitrary unit. Data are represented as mean ± SD.

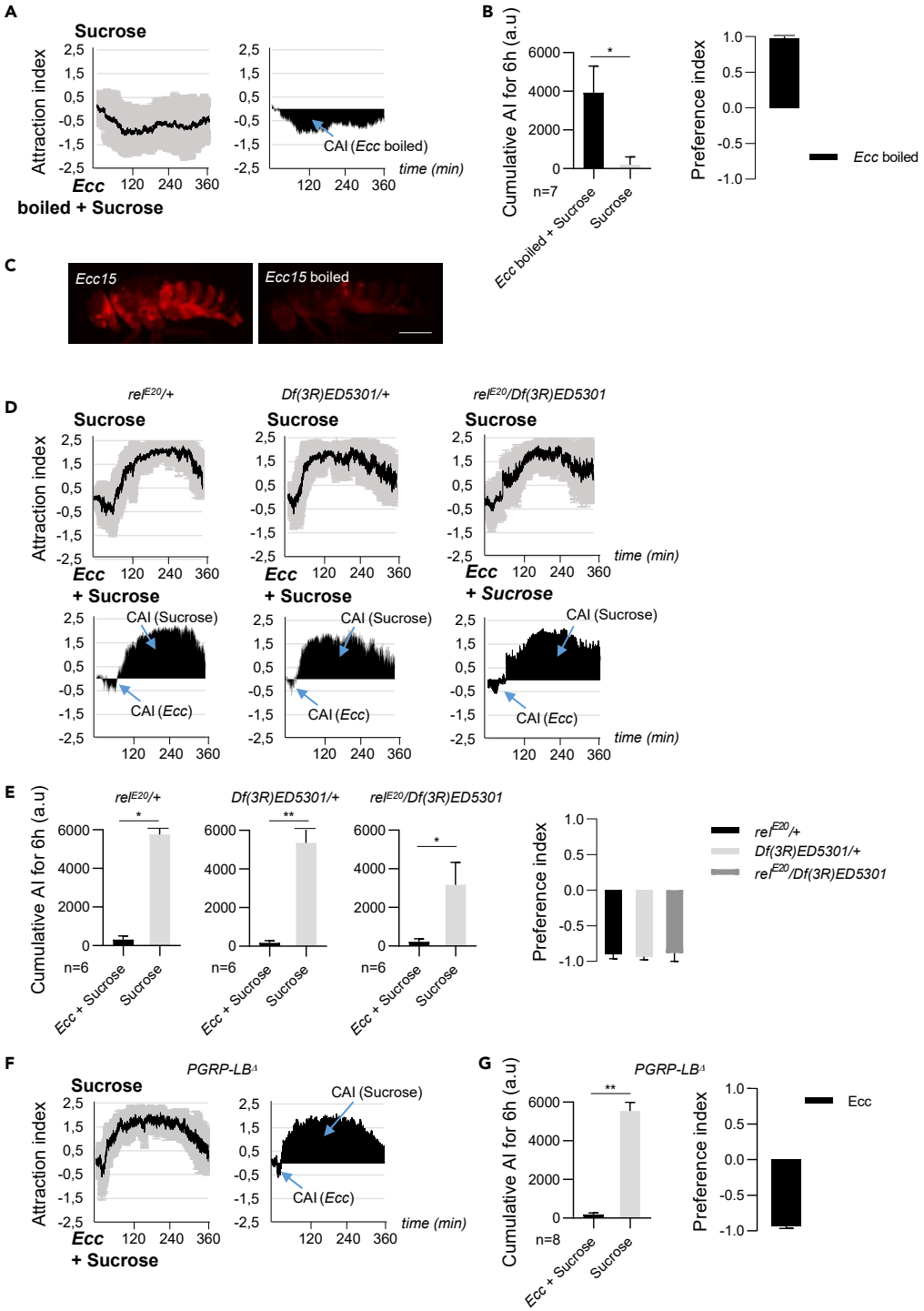

Figure 4. *Ecc* Aversion Does Not Require the IMD/NF-κB Signaling Pathway

(A and B) Heat-killed *Ecc* is no longer aversive to adult females. (A) (Top) Kinetics of the AI for sucrose when flies were given the choice between a heat-killed *Ecc* + sucrose versus sucrose-only solution. (Bottom) CAI area for each specified solution (arrows) and its distribution over time. (B) (Left): Histograms built with the CAI values from (A). *$p < 0.05$. Wilcoxon matched-pairs signed rank test, two-tailed p value. Error bars correspond to standard deviation. The reference index for boiled *Ecc* calculated with the CAI values from (A).

(C) PGRP-LB, *Diptericin-Cherry* flies fed for 24 h with either fresh (left) or boiled *Ecc* (right). Scale bar, 0.5 mm.

Figure 4. *Continued*

(D and E) *Relish* mutant flies behaved like controls. (D) (Top) Kinetics of the AI for sucrose when $rel^{E20}/Df(3R)ED5301$ flies and control $rel^{E20}/+$ and *Df(3R)ED5301/+* flies were given the choice between a *Ecc* + sucrose solution versus sucrose only. (Bottom) CAI area for each of the specified solution (arrows) and its distribution over time. (E) Histograms built with the CAI values from (D). *$p < 0.05$ and **$p < 0.01$. Wilcoxon matched-pairs signed rank test, two-tailed p value. Error bars correspond to standard deviation. The preference index for *Ecc* is calculated with the CAI values from (D).

(F and G) Flies mutant for the amidase PGRP-LB displayed a normal two-step behavior regarding *Ecc*. (F) (Right) Kinetics of the AI for sucrose when $PGRP\text{-}LB^{\Delta}$ flies were given the choice between an *Ecc* + sucrose solution versus sucrose only. (Left) CAI area for each specified solution (arrows) and its distribution over time. (G) Histograms built with the CAI values from (F). **$p < 0.01$. Wilcoxon matched-pairs signed rank test, two-tailed p value. Error bars correspond to standard deviation. The preference index for *Ecc* is calculated with the CAI values from (F). For (A and F) left graphs and (D) top graphs, the black lines and the gray lines correspond, respectively, to the mean and the standard deviation, and for (A and D) right graphs and (C) bottom graphs, solely the mean value of the CAI obtained with multiple replicates is shown in black. n indicates the number of experimental replicates. a.u.: arbitrary unit. Data are represented as mean ± SD.

$relish^{E20}$ mutant flies behaved as controls, showing the stereotyped two-phase compartment with an initial attraction to *Ecc* followed by a constant aversion to it (Figures 4D and 4E). Finally, to exclude the possibility that bacterial PGN affects the flies' feeding behavior independently of IMD signaling activation, we examined the feeding behavior of fly mutant for the amidase PGRP-LB, an enzyme that cleaves PGN fragments into non-immunogenic neuropeptides (Zaidman-Remy et al., 2006). We found no substantial differences between wild-type and flies mutant for the $PGRP\text{-}LB^{\Delta}$ null allele in our experimental setup (Figures 4F and 4G). Altogether, these results suggested that neither bacterial PGN nor the NF-κB signaling contributes to the feeding choice regarding *Ecc* and that bacteria have to be alive to be aversive for *D. melanogaster*. As previous work has reported a gustatory-mediated avoidance of bacterial LPS via the TrpA1 channel, we asked whether LPS could also mediate the second aversive phase that we observed with *Ecc* (Soldano et al., 2016). Two results let us believe that LPS is not the aversive molecule that repulses flies when in contact with *Ecc*. First, as mentioned in previous sections, *E. coli* whose cell wall is also composed of LPS was not repulsive for flies. Second, we found that flies mutant for TrpA1 showed the same biphasic behavior toward *Ecc* that controls flies that carry a functional TrpA1 receptor (Figures S2E and S2F).

Bitter Neurons and Bitter Gustatory Receptors Gr66a and Gr33a Are Required for the Aversion to *Ecc*

In *D. melanogaster*, detection of non-volatile repellents is mediated by dedicated gustatory receptors such as Gr66a, Gr33a, or Gr32a, expressed by a set of gustatory receptor neurons (Scott, 2018). We found that inactivation of bitter Gr66a neurons by expressing Kir2.1, an inwardly rectifying K^+ channel, abolished the repugnance to *Ecc* without affecting the initial attractive phase (Figures 5A and 5B) (Shim et al., 2015). Flies expressing *UAS-Kir2.1* under the control of $Gr66a^{Gal4}$ did not show any aversion to *Ecc* but were instead constantly feeding on the bacteria-containing solution until there was no more bacterial solution to feed on (Figures 5A and 5B). Furthermore, we found that the gustatory receptors Gr66a and Gr33a were both required for the aversion to *Ecc* (Moon et al., 2009; Video S3). Flies mutant for any of the two receptors displayed abnormal behavior, as they stayed close to the *Ecc* drop during most of the time with a high cumulative AI for *Ecc* (Figures 5C and 5D).

Having shown that Gr66a-expressing neurons are functionally required for *Ecc* avoidance, we wondered whether this effect was mediated by direct activation of these neurons by bacteria. To do so, we took advantage of the Ca-LexA (calcium-dependent nuclear import of LexA) technique that indirectly assesses Ca+ release in neurons that express the mLexA-VP16-NFAT fusion protein (Masuyama et al., 2012). When *LexAop-CD8-GFP-2A-CD8-GFP; UAS-mLexA-VP16-NFAT, lexAop-rCD2-GFP/*$Gr66a^{Gal4}$ flies were fed 4 days with an *Ecc*-contaminated solution, activation of the Ca-LexA reporter was detected in the sub-esophageal zone (SEZ) of the central brain, where peripheral nervous system (PNS) bitter neuron projections are found (Figure S3A). Flies fed with *E. coli*, boiled *Ecc,* or sucrose only showed weak or no Ca-LexA activation in that brain region (Figure S3A). No Ca-LexA signal was observed in Lk^{Gal4}, *LexAop-CD8-GFP-2A-CD8-GFP; UAS-mLexA-VP16-NFAT, lexAop-rCD2-GFP Ecc*-fed flies, showing the specificity of Ca-LexA results (Figure S3B). Altogether, these experiments indicated that flies are able to sense the presence of *Ecc* via bitter gustatory neurons. They also showed that these neurons are necessary to trigger an avoidance behavior toward these bacteria.

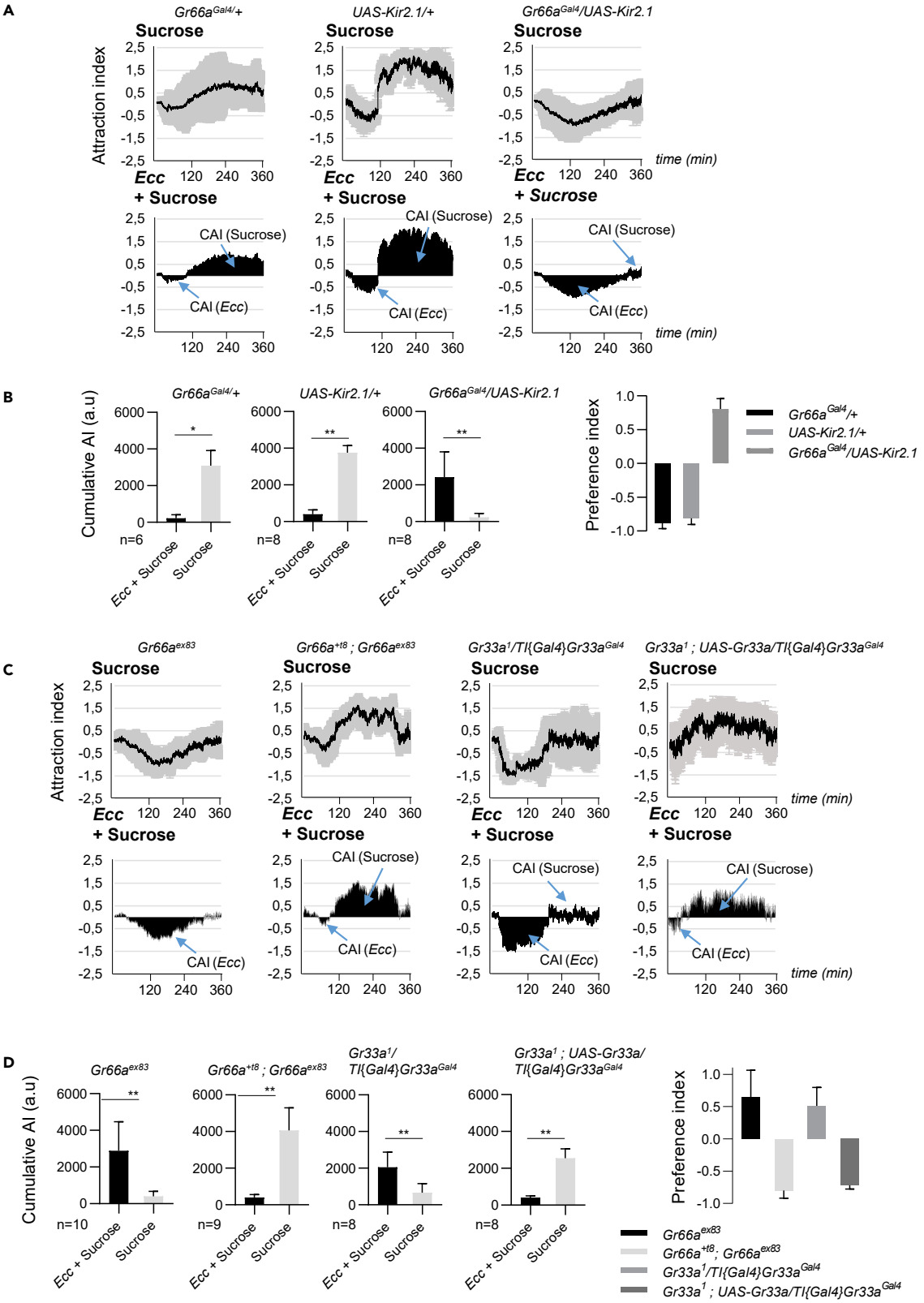
A
Gr66a Gal4/+
UAS-Kir2.1/+
Gr66a Gal4/UAS-Kir2.1
Sucrose
Attraction index
time (min)
Ecc
+ Sucrose
CAI (Sucrose)
CAI (Ecc)
B
Cumulative AI (a.u)
n=6
n=8
Ecc + Sucrose
Sucrose
Preference index
C
Gr66a ex83
Gr66a +t8 ; Gr66a ex83
Gr33a 1/TI{Gal4}Gr33a Gal4
Gr33a 1 ; UAS-Gr33a/TI{Gal4}Gr33a Gal4
D
n=10
n=9

Figure 5. Bitter Neurons and Bitter Gustatory Receptors Gr66a and Gr33a Are Required for the Aversion to *Ecc*

(A and B) Adult females expressing *UAS-Kir2.1* in bitter neurons using $Gr66a^{Gal4}$ displayed no aversion to *Ecc*, whereas control *UAS-Kir2.1/+* or $Gr66^{Gal4}$/+ did. (A) (Top) Kinetics of the AI for sucrose. (Bottom) CAI area for each specified solution (arrows) and its distribution over time. (B) Histograms built with the CAI values from (A). *p < 0.05 and **p < 0.01. Wilcoxon matched-pairs signed rank test, two-tailed p value. Error bars correspond to standard deviation. The preference index for *Ecc* is calculated with the CAI from (B).

(C and D) The gustatory receptors Gr66a and Gr33a are required for the aversion to *Ecc*. $Gr66^{ex83}$ or $Gr33a^{1}$/*TI{Gal4}*$Gr33a^{Gal4}$ mutant flies, but not rescue $Gr66^{+t8}$; $Gr66^{ex83}$ or $Gr33a^{1}$, *UAS-Gr33a/TI{Gal4}*$Gr33a^{Gal4}$ flies, displayed attraction but no aversion to *Ecc* when given the choice between an *Ecc*-contaminated sucrose solution versus sucrose only. (C) (Top) Kinetics of the AI for sucrose. (Bottom) CAI area for each specified solution (arrows) and its distribution over time. (D) Histograms built with the CAI values from (C). **p < 0.01. Wilcoxon matched-pairs signed rank test, two-tailed p value. Error bars correspond to standard deviation. The preference indexes for *Ecc* are calculated with the CAI values from (E). For (A and C) (top), the black lines and the gray lines correspond, respectively, to the mean and the standard deviation, and for bottom graphs, solely the mean value of the CAI obtained with multiple replicates is shown in black. n indicates the number of experimental replicates. a.u.: arbitrary unit. Data are represented as mean ± SD.

The Neuropeptide Leukokinin Is Required for the Aversive Perception of *Ecc*

Given that *Ecc* avoidance by adult flies was not immediate and occurred only after flies had ingested the bacteria-contaminated solution, we wondered which mechanism could contribute to this delayed *Ecc*-induced behavior. Neuropeptides, which are known to influence neuronal activities at a relatively low timescale (seconds to hours) compared with neurotransmitters (milliseconds), are good candidates to mediate the switch from attraction to aversion. Lk has been shown to modify the feeding behavior toward sucrose from attraction to aversion in the mosquito (Kwon et al., 2016). We, therefore, asked whether *D. melanogaster* Lk could be involved in the switch of fly behavior from attraction to repulsion when in contact with *Ecc*. Flies homozygotes for the hypomorphic allele Lk^{C275} or transheterozygotes Lk^{C275}/*Df(3L) Exel6123* were no longer avoiding the feeding solution contaminated by *Ecc* (Figures 6A–6C and Video S4), whereas control flies still did. This aberrant behavior of Lk^{C275} mutant flies was rescued by expressing *UAS-Lk* under the control of the Lk^{Gal4} driver (Figures S4A–S4C). These results demonstrated that the production of the neuropeptide Lk, by Lk^{Gal4}-expressing cells, is required for optimal avoidance of *Ecc*.

We found that Lk^{Gal4} is expressed in the adult central nervous system (Figure S5A), with some cells sending projections to the SEZ where gustatory information relay might occur. Thus, because $Gr66a^{Gal4}$- and Lk^{Gal4}-expressing cells were both required, although at a different level, for the *Ecc* gustatory repellent phenotype, we asked whether these two populations of cells share some common cells by focusing on the SEZ region of the central brain. Using an intersectional expression approach, we found that none of the $Gr66a^{Lexa}$-positive axons correspond to the Lk^{Gal4} ones (Figure S5B). However, we observed that the Lk^{Gal4} projections localized in the vicinity of axonal projections of bitter gustatory neurons labeled by $Gr32a^{Lexa}$ (Figure S5A).

The Latency before Repulsion Requires Depotentiation of Bitter Taste

As for most of the tests used to analyze fly behavior upon feeding, our experimental paradigm requires that we used starved flies. However, nutrient deprivation can lead to dramatic changes in feeding behavior, including acceptance of foods that are normally rejected. Bitter substances are more acceptable, and sweet molecules less attractive for starved than for fed flies (Freeman and Dahanukar, 2015; LeDue et al., 2016). As we used starved flies in our experiments, we asked whether the attractive and/or the aversion phases were dependent on the fly feeding status. To appreciate the influence of starvation to the results of our test, we performed it with non-starved flies (Figures 7A and 7B). In this case, the attraction phase was completely lost and the repulsive phase was very slowly and progressively established. This behavioral shift could depend in part on reciprocal sensitization and desensitization of sweet and bitter tastes (Inagaki et al., 2014; LeDue et al., 2016). Good candidates to mediate this effect are the neuropeptides NeuroPeptide F (NPF) that control reciprocal changes in sweet and bitter sensitivity during starvation. dNPF+ neurons promote increased sugar sensitivity, whereas sNPF neurons promote decreased bitter sensitivity (Inagaki et al., 2014). However, as sNPF mutant flies behaved as controls in our behavior test, we excluded sNPF implication in *Ecc* perception (Figures S6A and S6B). Previous works have also identified a set of neurons (named OA-VL) in which starvation induces a reduction of octopamine production leading to Gr66a bitter taste neuron depotentiation (LeDue et al., 2016). Consistent with this model, artificial silencing of octopamine and/or tyramine activity in these neurons induces a starvation-like reduction in bitter sensory neuron output. To test if the attraction of starved flies to *Ecc* was also dependent by this OA-VL module, we recorded the behavior of flies in which the octopamine receptor Oct-TyrR was genetically down-regulated in Gr66a neurons. In contrast to parental strains that behaved as controls, progeny having reduced octopamine signaling in bitter neurons were attracted by *Ecc* (Figures 7C and 7D). However, in this case

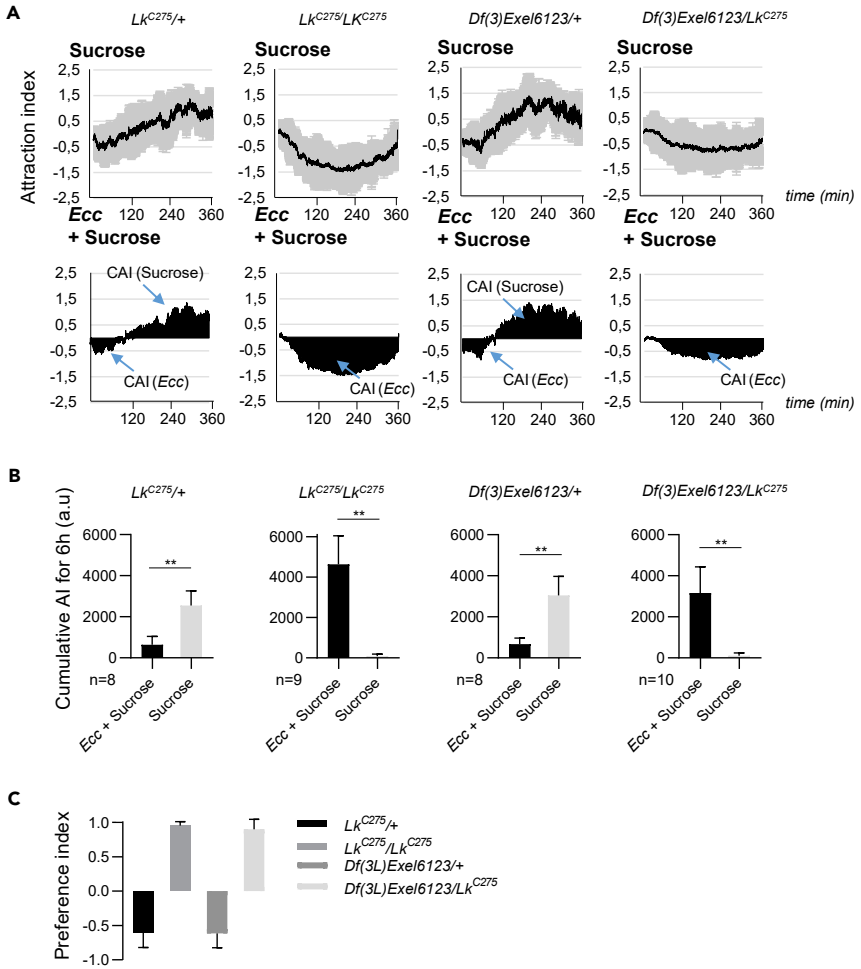

Figure 6. The Neuropeptide Leukokinin Is Required for the Aversive Perception of *Ecc*

(A and B) Flies homozygous for the hypomorphic allele Lk^{C275} or transheterozygotes $Lk^{C275}/Df(3L)\ Exel6123$ no longer avoided the feeding solution contaminated by *Ecc*, whereas control flies ($Lk^{C275}/+$ and *Df(3L) Exel6123/+*) did, when females were given the choice between an *Ecc*-contaminated sucrose solution versus sucrose only. (A) (Top) Kinetics of the AI for sucrose. (Bottom) CAI area for each specified solution (arrows) and its distribution over time. (B) Histograms built with the CAI values from (A). $^{**}p < 0.01$. Wilcoxon matched-pairs signed rank test, two-tailed p value. Error bars correspond to standard deviation.

(C) Preference indexes for *Ecc* calculated with the CAI from (B). For (A) top graphs, the black lines and the gray lines correspond, respectively, to the mean and the standard deviation, and for bottom graphs, solely the mean value of the CAI obtained with multiple replicates is shown in black. n indicates the number of experimental replicates. a.u.: arbitrary unit. Data are represented as mean ± SD.

the attraction phase lasted longer than for control flies, and hence the repulsive phase started later. These results suggested a model in which starved flies that have highly depotentialized bitter neurons do not perceive the "bitterness" of *Ecc* and fed on it. They prefer *Ecc* to sucrose only because the bacteria solution has probably a higher nutrient value for them than sucrose-only solution. Once the flies are fed by bacteria, their starvation status progressively decreases together with bitter neuron depotentiation. In bacteria-fed flies, the bitter neurons are no longer silenced and progressively sense the bitterness of *Ecc*, and hence flies begin to avoid it. To further test this hypothesis, we performed the experiments with progressively diluted *Ecc* solutions. We hypothesized that diluted *Ecc* solutions will be less nutritive than concentrated ones. If such, bitter neuron potentiation should take longer and the attraction phase length should last longer with diluted *Ecc* solutions. Our results showed that the more diluted the bacterial solution is, the longer the duration of the attraction phase lasted and the more the repulsive phase was delayed. For the highest diluted *Ecc* solutions (32× and 64×), the repulsive phase was even shorter

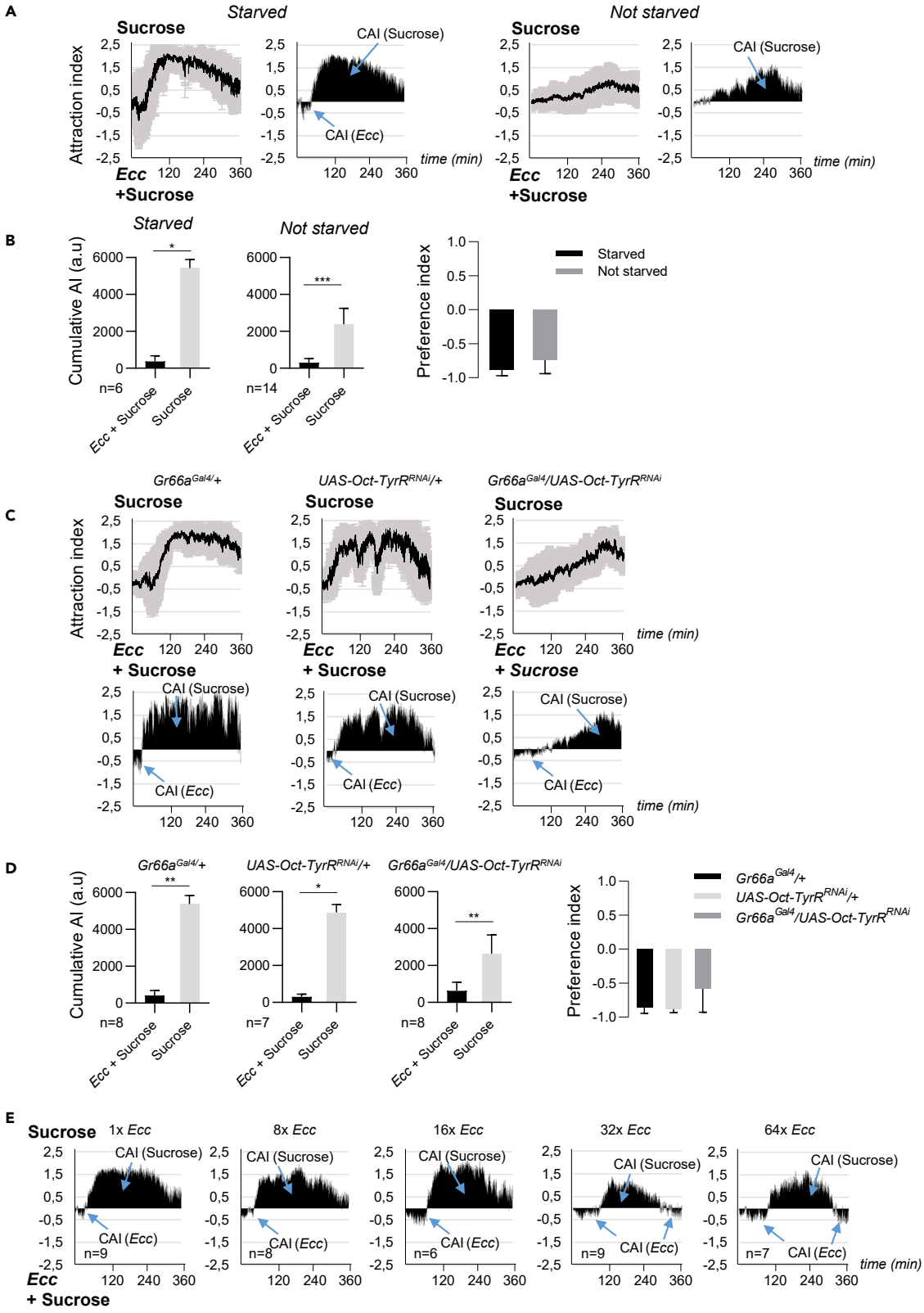
A
Starved
Not starved
Sucrose
Attraction index
CAI (Sucrose)
CAI (Ecc)
time (min)
Ecc
+Sucrose
B
Starved
Not starved
Cumulative AI (a.u)
n=6
n=14
Ecc + Sucrose
Sucrose
Preference index
Starved
Not starved
C
Gr66a^Gal4/+
UAS-Oct-TyrR^RNAi/+
Gr66a^Gal4/UAS-Oct-TyrR^RNAi
Sucrose
Attraction index
Ecc
+ Sucrose
CAI (Sucrose)
CAI (Ecc)
time (min)
D
Gr66a^Gal4/+
UAS-Oct-TyrR^RNAi/+
Gr66a^Gal4/UAS-Oct-TyrR^RNAi
Cumulative AI (a.u)
n=8
n=7
n=8
Ecc + Sucrose
Sucrose
Preference index
E
Sucrose
1x Ecc
8x Ecc
16x Ecc
32x Ecc
64x Ecc
CAI (Sucrose)
CAI (Ecc)
n=9
n=8
n=6
n=9
n=7
Ecc
+ Sucrose
time (min)

Figure 7. Starvation and Depotentiation of Bitter Neurons Delay Aversion to *Ecc*

(A and B) Non-starved flies displayed reduced attraction and aversion to *Ecc*. (A) (Left graphs) Kinetics of the AI for sucrose when starved flies or non-starved flies were given the choice between an *Ecc*-contaminated sucrose solution versus sucrose only. (Right graphs) CAI area for each specified solution (arrows) and its distribution over time. (B) Histograms built with the CAI values from (A). *p < 0.05 and ***p < 0.001. Wilcoxon matched-pairs signed rank test, two-tailed p value. Error bars correspond to standard deviation. The preference indexes for *Ecc* are calculated with the CAI values from (A). For (A) left graphs and (C) top graphs, the black lines and the gray lines correspond, respectively, to the mean and the standard deviation, and for (A) left graphs and (C) bottom graphs, solely the mean value of the CAI obtained with multiple replicates is shown in black.

(C and D) Adult females expressing *UAS-Oct-TyrR*^{RNAi} in bitter neurons using *Gr66a*^{Gal4} displayed prolonged attraction and delayed aversion to *Ecc*, whereas control *UAS- Oct-TyrR*^{RNAi}/+ or *Gr66*^{Gal4}/+ do not. (C) (Top) Kinetics of the AI for sucrose. (Bottom) CAI area for each specified solution (arrows) and its distribution over time. (D) Histograms built with the CAI values from (C). *p < 0.05 and **p < 0.01. Wilcoxon matched-pairs signed rank test, two-tailed p value. Error bars correspond to standard deviation. The preference indexes for *Ecc* are calculated with the CAI from (D).

(E) Increased attraction to *Ecc* and delayed repulsion to *Ecc* when using diluted bacteria solutions. CAI area for each specified solution (arrows) and its distribution over time when flies are given the choice between an *Ecc*-contaminated sucrose solution of the indicated dilution (1× to 64×) versus sucrose only. For (A) left graphs and (C) top graphs, the black lines and the gray lines correspond, respectively, to the mean and the standard deviation, and for (A) right graphs and (C) bottom graphs, solely the mean value of the CAI obtained with multiple replicates is shown in black. n indicates the number of experimental replicates. a.u.: arbitrary unit. Data are represented as mean ± SD.

followed by a novel attractive phase (Figure 7E). These data suggest that *Ecc* has a higher nutrient value for the flies than sucrose only. For the highly diluted bacterial solutions, this nutrient value is not strong enough to maintain the flies in a fed status for the entire experiment. After a certain time, the flies enter a novel phase of starvation and are therefore again attracted by *Ecc*.

Behaviors toward *Ecc* Are Bacterial and Fly Species Specific

To analyze the universality of the above-described phenomena, we tested the fly feeding behavior toward sucrose solution contaminated with other DAP-type PGN, such *E. coli*, *Lactobacillus plantarum*, or *Acetobacter pomorum* the latter two being commensal bacteria that have been shown to colonize *Drosophila* gut (Sharon et al., 2011; Storelli et al., 2011). Both *E. coli* and *L. plantarum* species were clearly attractive for female flies, PI (*E. coli*) = 0.89 ± 0.11 SD et PI (*L. plantarum*) = 0.94 ± 0.16 SD, whereas *A. pomorum* was equally preferred (PI (*A. pomorum*) = -0.02 ± 0.32 SD) but with a long attraction phase. The second aversive phase observed with *Ecc* was not present with the three species (Figures S7A–S7F). This showed that although flies are attracted by bacteria in general, the subsequent aversive phase is specific to *Ecc*.

We next wanted to test whether the stereotyped behavior toward *Ecc* was conserved among different Drosophilidae. Interestingly, whereas the biphasic behavior was also observed for *Drosophila biarmipes*, it was not when its closely related species *Drosophila suzukii* was used for the tow-choice assay (Figures S8A–S8C). Indeed, we observed that *Ecc* was not aversive and only slightly attractive for *D. suzukii*. A similar pattern was observed for *Drosophila ananassae*. The absence of yet available genetic tools in *D. biarmipes* prevented us to test whether the cues and sensory systems at play to mediate this bacteria-fly interaction are the same in *D. biarmipes* and *D. melanogaster*, two phylogenetically distant species.

DISCUSSION

Our results demonstrate that *Ecc* is perceived as bitter by the flies that are therefore repulsed by it. This repulsive phase, which takes around 1 h to be established, depends on Gr66a-positive neurons (Figure 8). One bacterial product candidate to trigger the repulsive behavior is the cell wall LPS, which has been shown to be perceived as bitter by *D. melanogaster* in a TRPA1-dependent manner (Soldano et al., 2016). However, we do not believe that, in our assay, LPS is the bitter substance. Indeed, *E. coli* whose cell wall also contains LPS was not repulsive to flies. In addition, *TrpA1* mutant flies, which are supposed to be LPS insensitive, were as repulsed as control flies by *Ecc*. The use of live bacteria that are probably sensed via multiple cues instead of an LPS solution as in the Soldano et al. studies might explain these discrepancies. Besides, as the structure of LPS and its recognition by *ad hoc* pattern recognition receptor(s) are highly bacterial species dependent, different bacterial LPS might trigger different responses via different receptors. It should also be noted that the repulsive phase is Orco-independent indicating that Geosmin and phenol, two olfactory cues previously shown to mediate bacteria avoidance, are probably not involved in this behavior (Mansourian et al., 2016; Stensmyr et al., 2012).

The data obtained with bitter Gr mutant and Ca-LexA suggested that flies can sense bacteria bitterness after being in contact with them. One puzzling result of this study is the latency of around 1 h that is required

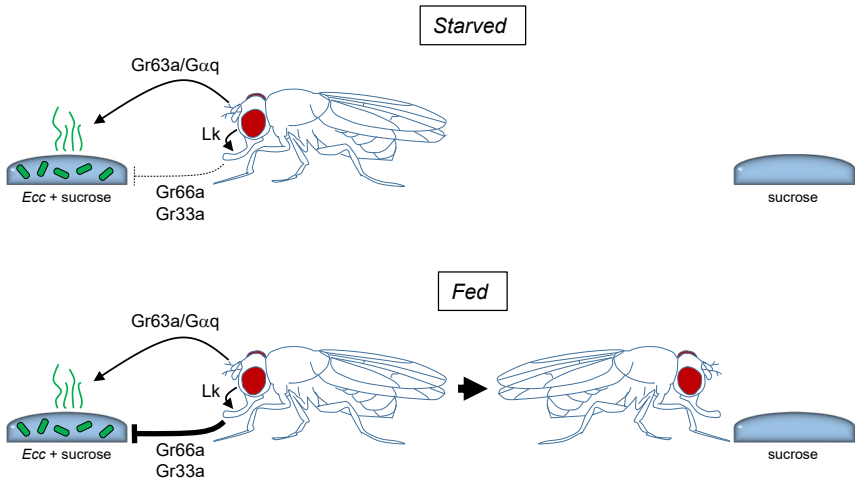

Figure 8. Model for the Role of the Olfactory and Gustatory Modalities in the Biphasic Behavior of Adult Flies in Response to *Ecc*

Starved flies are first attracted by odors emanating from the *Ecc*-contaminated solution. This step requires both the olfactory receptor Gr63a, expressed by the CO_2-sensing neurons hosted by the antenna, and the Gαq1 transducer. Starved flies have reduced bitter sensitivity due to Gr66a/Gr33a-expressing neuron depotentiation. Feeding on the sucrose + *Ecc*-contaminated solution induces the re-potentiation of bitter neurons. No longer potentiated, the bitter neurons established an aversive behavior toward *Ecc*. The gustatory receptors Gr66a and Gr33a, expressed by the bitter neurons of the labellum and of the tarsae, are required for this second phase. The neuropeptide Lk expressed by the central nervous system is also required for optimal aversion.

for the repulsive phase to be consolidated. A few reasons let us hypothesize that this phase requires that bacteria are internally sensed by the flies and that bacteria-derived PGN could be the mediator of the effect. First, in contrast to *E. coli* and *L. plantarum*, which were not repulsive in our assay, gut-associated *Ecc* was shown to release PGN that can reach fly blood where it interacts with both immune and neuronal tissues. The ability of *Ecc* to activate fly immunity, to modify fly egg-laying behavior, and to be perceived as bitter are all dependent on using live bacteria because they are abolished when *Ecc* is heat killed (Basset et al., 2000; Kurz et al., 2017). Finally, at the time *Ecc* was avoided by the flies, it was present in the intestinal tract. One could propose that internal sensing of gut-born *Ecc* PGN translocated to the hemolymph could explain the 1-h delay between attraction and repulsion. However, our data using flies mutant for the NF-κB transcription factor Relish downstream of the main gram-negative bacteria immune cascade IMD indicate that PGN sensing that mediates both immune and behavioral responses to bacteria is involved neither in the attractive nor in the repulsive phase. Consistently, *PGRP-LB*$^{\Delta}$ mutant in which both immune and behavior responses to *Ecc* are exacerbated presented the same comportment as controls when given the choice between sucrose and *Ecc*.

Our results demonstrate that non-starved flies are more repulsed by *Ecc* let us propose another model to explain the delayed response. In starved flies, reduced octopamine signaling promotes depotentiation of bitter neurons. *Ecc* produce bitter substances that are not sensed by the bitter pathway because of its depotentiation. As flies feed on *Ecc*, their starvation status is progressively decreased, bitter neuron depotentiation is lost, and *Ecc* bitterness is perceived again. These data suggest that bacteria can be a source of food for the flies, which is consistent with previous reports (Yamada et al., 2015). The fact that the other bacterial species tested are attractive but not repulsive for the flies suggests that they also are a source of food but do not produce substances that are bitter for the flies.

Our data showed that, in the presence of *Ecc*, *D. melanogaster* were attracted to the bacteria-contaminated solution. The fact that *Orco* minus flies still preferred *Ecc*-contaminated over sucrose solution suggested that other odors/Rc complexes were implicated in this attractive phase or other sensory modalities such as gustation contributed to the initial attraction (Becher et al., 2018). Ionotropic receptors that sense odors in an Orco-independent manner are good candidates to mediate the effect (Gomez-Diaz et al.,

2018). Although we do not know what is the nature of the attractive substance produced by *Ecc*, our results clearly demonstrate that this attraction mediates its effects via the CO_2 receptor Gr63a and the Gαq transducer. Our results suggest that, as it has been shown for spermidine, *Ecc* produces a yet unknown compound that inhibits the CO_2 receptor neurons and that inhibition of this avoidance pathway is necessary for attraction toward *Ecc*.

The present work demonstrated that the behavior of different *Drosophila* species toward *Ecc* is not generic but rather species specific. *D. melanogaster* is a vector for this potato blackleg bacterium by transmitting it from contaminated to healthy plants (Czajkowski et al., 2015). It would be interesting to know whether *D. biarmipes*, which presented a similar behavioral profile, is also a vector for *Ecc*. It is also clear that the persistent presence of *Ecc* in *D. melanogaster* had deleterious effects on the host, some of them being mediated by the PGN/NF-κB module (Lee and Ferrandon, 2011). This biphasic mode of interaction with *Ecc*, with an initial attractive phase rapidly followed by a repulsive one, would allow *D. melanogaster*-mediated *Ecc* dispersion on plants without affecting the integrity of the host due to an overprolonged contact with the bacteria.

Limitations of the Study

Although we have shown that *Ecc* is perceived as bitter by *D. melanogaster*, we have not identified the exact compound(s) that repulse the flies. Similarly, we have not uncovered what initially attracted starved flies to the *Ecc*-contaminated solution. If our data speak for a role of Gr66a bitter neurons and Lk in *D. melanogaster* aversion toward *Ecc*, we are missing a putative functional link between them. Finally, we do not know whether GR63a and Gαq1 act in a linear signaling pathway to control *D. melanogaster* attraction to *Ecc*.

Resource Availability

Lead Contact

Further information and requests for resources and reagents should be directed to and will be fulfilled by the lead contact, Julien Royet (Julien.royet@univ-amu.fr).

Materials Availability

All unique/stable reagents generated in this study will be made available on request.

Data and Code Availability

The original/source data are available from the lead contact on request.

METHODS

All methods can be found in the accompanying Transparent Methods supplemental file.

SUPPLEMENTAL INFORMATION

Supplemental Information can be found online at https://doi.org/10.1016/j.isci.2020.101152.

ACKNOWLEDGMENTS

We thank Sabine Peslier for technical help. This work was supported by (ANR-11-LABX-0054) (Investissements d'Avenir–Labex INFORM), ANR BACNEURODRO (ANR-17-CE16-0023-01) and ANR PEPTIMET (ANR-18-CE15-0018-02), Equipe Fondation pour la Recherche Médicale (EQU201903007783), and l'Institut Universitaire de France to J.R.

AUTHOR CONTRIBUTIONS

Conceptualization, B.C., F.D., and J.R.; Methodology, B.C. and F.D.; Investigation, B.C.; Formal analysis, B.C. and F.D.; Writing – Original Draft, B.C. and J.R.; Writing – Review & Editing, B.C. and J.R.; Funding Acquisition, J.R.; Supervision, B.C. and J.R.

DECLARATION OF INTERESTS

The authors declare no competing interests.

CellPress
OPEN ACCESS

Received: October 7, 2019
Revised: March 2, 2020
Accepted: May 6, 2020
Published: June 26, 2020

REFERENCES

Acosta Muniz, C., Jaillard, D., Lemaitre, B., and Boccard, F. (2007). Erwinia carotovora Evf antagonizes the elimination of bacteria in the gut of Drosophila larvae. Cell. Microbiol. *9*, 106–119.

Basset, A., Khush, R.S., Braun, A., Gardan, L., Boccard, F., Hoffmann, J.A., and Lemaitre, B. (2000). The phytopathogenic bacteria Erwinia carotovora infects Drosophila and activates an immune response. Proc. Natl. Acad. Sci. U S A *97*, 3376–3381.

Becher, P.G., Lebreton, S., Wallin, E.A., Hedenstrom, E., Borrero, F., Bengtsson, M., Joerger, V., and Witzgall, P. (2018). The scent of the fly. J. Chem. Ecol. *44*, 431–435.

Bergman, P., Seyedoleslami Esfahani, S., and Engstrom, Y. (2017). Drosophila as a model for human diseases-focus on innate immunity in barrier epithelia. Curr. Top. Dev. Biol. *121*, 29–81.

Bosco-Drayon, V., Poidevin, M., Boneca, I.G., Narbonne-Reveau, K., Royet, J., and Charroux, B. (2012). Peptidoglycan sensing by the receptor PGRP-LE in the Drosophila gut induces immune responses to infectious bacteria and tolerance to microbiota. Cell Host Microbe *12*, 153–165.

Buchon, N., Broderick, N.A., Poidevin, M., Pradervand, S., and Lemaitre, B. (2009). Drosophila intestinal response to bacterial infection: activation of host defense and stem cell proliferation. Cell Host Microbe *5*, 200–211.

Buchon, N., Silverman, N., and Cherry, S. (2014). Immunity in Drosophila melanogaster–from microbial recognition to whole-organism physiology. Nat. Rev. Immunol. *14*, 796–810.

Capo, F., Charroux, B., and Royet, J. (2016). Bacteria sensing mechanisms in Drosophila gut: local and systemic consequences. Dev. Comp. Immunol. *64*, 11–21.

Charroux, B., Capo, F., Kurz, C.L., Peslier, S., Chaduli, D., Viallat-Lieutaud, A., and Royet, J. (2018). Cytosolic and secreted peptidoglycan-degrading enzymes in Drosophila respectively control local and systemic immune responses to microbiota. Cell Host Microbe *23*, 215–228.e4.

Czajkowski, R., Perombelon, M., Jafra, S., Lojkowska, E., Potrykus, M., van der Wolf, J., and Sledz, W. (2015). Detection, identification and differentiation of Pectobacterium and Dickeya species causing potato blackleg and tuber soft rot: a review. Ann. Appl. Biol. *166*, 18–38.

Douglas, A.E. (2014). The molecular basis of bacterial-insect symbiosis. J. Mol. Biol. *426*, 3830–3837.

Freeman, E.G., and Dahanukar, A. (2015). Molecular neurobiology of Drosophila taste. Curr. Opin. Neurobiol. *34*, 140–148.

Gomez-Diaz, C., Martin, F., Garcia-Fernandez, J.M., and Alcorta, E. (2018). The two main olfactory receptor families in Drosophila, ORs and IRs: a comparative approach. Front. Cell. Neurosci. *12*, 253.

Haller, S., Limmer, S., and Ferrandon, D. (2014). Assessing Pseudomonas virulence with a nonmammalian host: Drosophila melanogaster. Methods Mol. Biol. *1149*, 723–740.

Inagaki, H.K., Panse, K.M., and Anderson, D.J. (2014). Independent, reciprocal neuromodulatory control of sweet and bitter taste sensitivity during starvation in Drosophila. Neuron *84*, 806–820.

Jones, W.D., Cayirlioglu, P., Kadow, I.G., and Vosshall, L.B. (2007). Two chemosensory receptors together mediate carbon dioxide detection in Drosophila. Nature *445*, 86–90.

Kapsetaki, S.E., Tzelepis, I., Avgousti, K., Livadaras, I., Garantonakis, N., Varikou, K., and Apidianakis, Y. (2014). The bacterial metabolite 2-aminoacetophenone promotes association of pathogenic bacteria with flies. Nat. Commun. *5*, 4401.

Kleino, A., and Silverman, N. (2014). The Drosophila IMD pathway in the activation of the humoral immune response. Dev. Comp. Immunol. *42*, 25–35.

Kurz, C.L., Charroux, B., Chaduli, D., Viallat-Lieutaud, A., and Royet, J. (2017). Peptidoglycan sensing by octopaminergic neurons modulates Drosophila oviposition. Elife *6*, e21937.

Kwon, H., Ali Agha, M., Smith, R.C., Nachman, R.J., Marion-Poll, F., and Pietrantonio, P.V. (2016). Leucokinin mimetic elicits aversive behavior in mosquito Aedes aegypti (L.) and inhibits the sugar taste neuron. Proc. Natl. Acad. Sci. U S A *113*, 6880–6885.

Kwon, J.Y., Dahanukar, A., Weiss, L.A., and Carlson, J.R. (2007). The molecular basis of CO2 reception in Drosophila. Proc. Natl. Acad. Sci. U S A *104*, 3574–3578.

LeDue, E.E., Mann, K., Koch, E., Chu, B., Dakin, R., and Gordon, M.D. (2016). Starvation-induced depotentiation of bitter taste in Drosophila. Curr. Biol. *26*, 2854–2861.

Lee, K.A., and Lee, W.J. (2014). Drosophila as a model for intestinal dysbiosis and chronic inflammatory diseases. Dev. Comp. Immunol. *42*, 102–110.

Lee, K.Z., and Ferrandon, D. (2011). Negative regulation of immune responses on the fly. EMBO J. *30*, 988–990.

Lestradet, M., Lee, K.Z., and Ferrandon, D. (2014). Drosophila as a model for intestinal infections. Methods Mol. Biol. *1197*, 11–40.

MacWilliam, D., Kowalewski, J., Kumar, A., Pontrello, C., and Ray, A. (2018). Signaling mode of the broad-spectrum conserved CO2 receptor is one of the important determinants of odor valence in Drosophila. Neuron *97*, 1153–1167.e4.

Mansourian, S., Corcoran, J., Enjin, A., Lofstedt, C., Dacke, M., and Stensmyr, M.C. (2016). Fecal-derived phenol induces egg-laying aversion in Drosophila. Curr. Biol. *26*, 2762–2769.

Masuyama, K., Zhang, Y., Rao, Y., and Wang, J.W. (2012). Mapping neural circuits with activity-dependent nuclear import of a transcription factor. J. Neurogenet. *26*, 89–102.

Moon, S.J., Lee, Y., Jiao, Y., and Montell, C. (2009). A Drosophila gustatory receptor essential for aversive taste and inhibiting male-to-male courtship. Curr. Biol. *19*, 1623–1627.

Nehme, N.T., Liegeois, S., Kele, B., Giammarinaro, P., Pradel, E., Hoffmann, J.A., Ewbank, J.J., and Ferrandon, D. (2007). A model of bacterial intestinal infections in Drosophila melanogaster. PLoS Pathog. *3*, e173.

Quevillon-Cheruel, S., Leulliot, N., Muniz, C.A., Vincent, M., Gallay, J., Argentini, M., Cornu, D., Boccard, F., Lemaitre, B., and van Tilbeurgh, H. (2009). Evf, a virulence factor produced by the Drosophila pathogen Erwinia carotovora, is an S-palmitoylated protein with a new fold that binds to lipid vesicles. J. Biol. Chem. *284*, 3552–3562.

Royet, J., Gupta, D., and Dziarski, R. (2011). Peptidoglycan recognition proteins: modulators of the microbiome and inflammation. Nat. Rev. Immunol. *11*, 837–851.

Scott, K. (2018). Gustatory processing in Drosophila melanogaster. Annu. Rev. Entomol. *63*, 15–30.

Sharon, G., Segal, D., Zilber-Rosenberg, I., and Rosenberg, E. (2011). Symbiotic bacteria are responsible for diet-induced mating preference in Drosophila melanogaster, providing support for the hologenome concept of evolution. Gut Microbes *2*, 190–192.

Shim, J., Lee, Y., Jeong, Y.T., Kim, Y., Lee, M.G., Montell, C., and Moon, S.J. (2015). The full repertoire of Drosophila gustatory receptors for detecting an aversive compound. Nat. Commun. *6*, 8867.

Soldano, A., Alpizar, Y.A., Boonen, B., Franco, L., Lopez-Requena, A., Liu, G., Mora, N., Yaksi, E., Voets, T., Vennekens, R., et al. (2016). Gustatory-mediated avoidance of bacterial lipopolysaccharides via TRPA1 activation in Drosophila. Elife *5*, e13133.

Stensmyr, M.C., Dweck, H.K., Farhan, A., Ibba, I., Strutz, A., Mukunda, L., Linz, J., Grabe, V., Steck, K., Lavista-Llanos, S., et al. (2012). A conserved

dedicated olfactory circuit for detecting harmful microbes in Drosophila. Cell *151*, 1345–1357.

Storelli, G., Defaye, A., Erkosar, B., Hols, P., Royet, J., and Leulier, F. (2011). Lactobacillus plantarum promotes Drosophila systemic growth by modulating hormonal signals through TOR-dependent nutrient sensing. Cell Metab. *14*, 403–414.

Turner, S.L., and Ray, A. (2009). Modification of CO2 avoidance behaviour in Drosophila by inhibitory odorants. Nature *461*, 277–281.

Vodovar, N., Vinals, M., Liehl, P., Basset, A., Degrouard, J., Spellman, P., Boccard, F., and Lemaitre, B. (2005). Drosophila host defense after oral infection by an entomopathogenic Pseudomonas species. Proc. Natl. Acad. Sci. U S A *102*, 11414–11419.

Yamada, R., Deshpande, S.A., Bruce, K.D., Mak, E.M., and Ja, W.W. (2015). Microbes promote amino acid harvest to rescue undernutrition in Drosophila. Cell Rep. *10*, 865–872.

Yao, C.A., and Carlson, J.R. (2010). Role of G-proteins in odor-sensing and CO2-sensing neurons in Drosophila. J. Neurosci. *30*, 4562–4572.

Yavuz, A., Jagge, C., Slone, J., and Amrein, H. (2014). A genetic tool kit for cellular and behavioral analyses of insect sugar receptors. Fly (Austin) *8*, 189–196.

Zaidman-Remy, A., Herve, M., Poidevin, M., Pili-Floury, S., Kim, M.S., Blanot, D., Oh, B.H., Ueda, R., Mengin-Lecreulx, D., and Lemaitre, B. (2006). The Drosophila amidase PGRP-LB modulates the immune response to bacterial infection. Immunity *24*, 463–473.

iScience, Volume *23*

Supplemental Information

Drosophila Aversive Behavior toward *Erwinia carotovora carotovora* Is Mediated by Bitter Neurons and Leukokinin

Bernard Charroux, Fabrice Daian, and Julien Royet

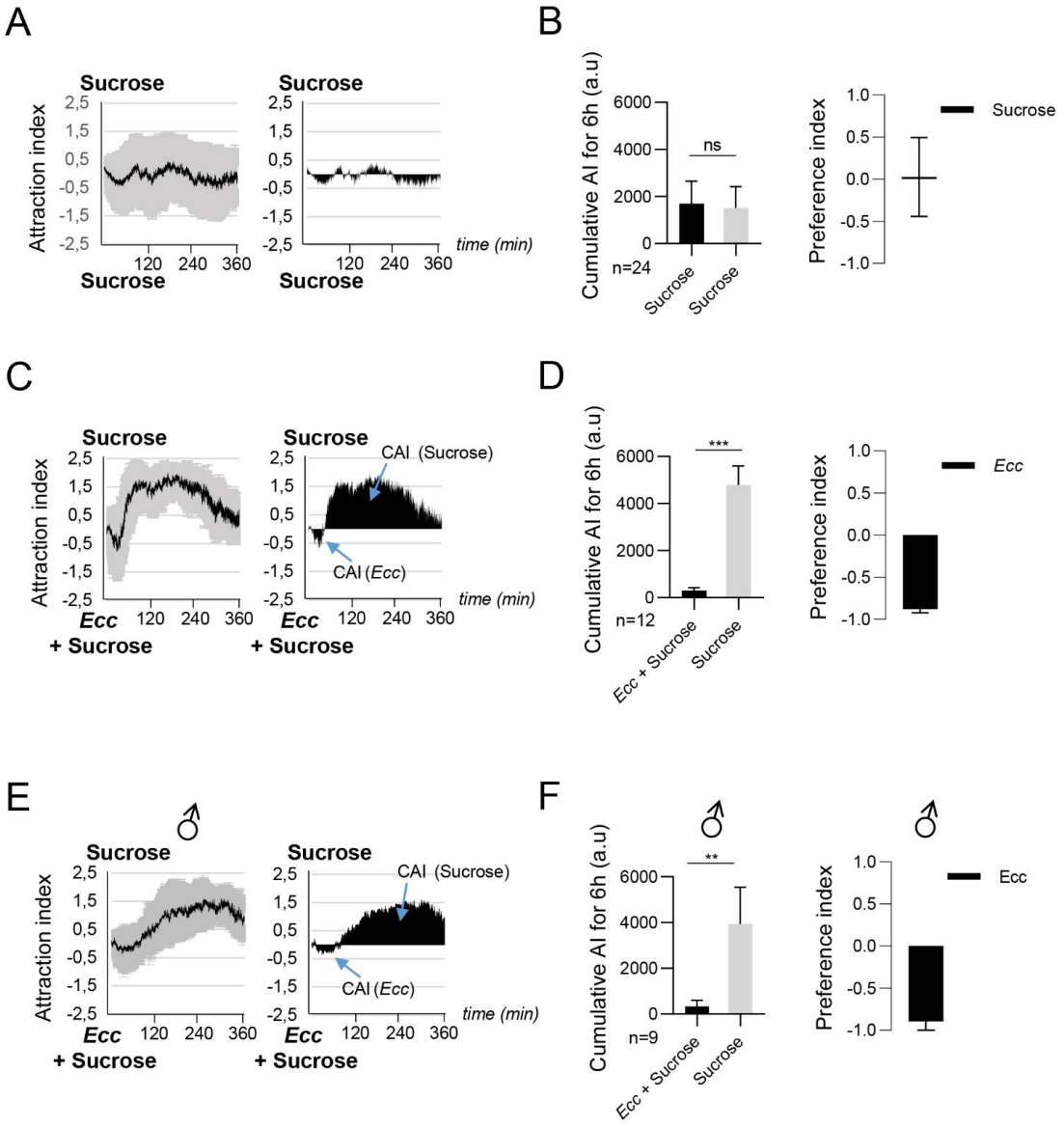

Figure S1. No directional bias in drop solution preference and *D. melanogaster* males behave as controls. Related to Figure 1.

A-B, No significant preference of adult females when given the choice between two identical 50mM sucrose solutions. A, (Left) Kinetic of the AI for sucrose in a sucrose versus sucrose experiment. (Right), CAI area for each sucrose solution and its distribution over time. B, (Left), histograms built with the CAI values from A. n.s: not significant. Wilcoxon matched-pairs signed-rank test, Two-tailed P value. Error bars correspond to standard deviation. The preference index for sucrose is calculated with the CAI values from B. C-D, Adult females displayed a two-step behavior when given the choice between an *Ecc* contaminated sucrose solution and a sucrose only solution of randomized position. C, (Left) Kinetic of the AI for sucrose in a sucrose versus sucrose + *Ecc* experiment. (Right), CAI area for each specified solution (arrows) and its distribution over time. D, (Left), histograms built with the CAI values from C.

*** P value< 0,001. Wilcoxon matched-pairs signed-rank test, Two-tailed P value. Error bars correspond to standard deviation. The preference index for *Ecc* is calculated with the CAI values from D. E-F, Adult males displayed a two-step behavior when given the choice between an *Ecc* contaminated sucrose solution versus sucrose only. E, (Left) Kinetic of the AI for Sucrose. Flies were first attracted by the bacteria solution before moving away from the contaminated solution. (Right) CAI area for each specified solution (arrows) and its distribution over time. F, Histograms built with the CAI values from E. ** P value< 0,01. Wilcoxon matched-pairs signed rank test, Two-tailed P value. Error bars correspond to standard deviation. The preference index for *Ecc* is calculated with the CAI values from F. For A, C and E left graphs, the black lines and the grey lines correspond respectively to the mean and the standard deviation, and for right graphs sole the mean value of the CAI obtained with multiple replicates is shown in black. n indicates the number of experimental replicates. a.u: arbitrary unit. Data are represented as mean +/- SD.

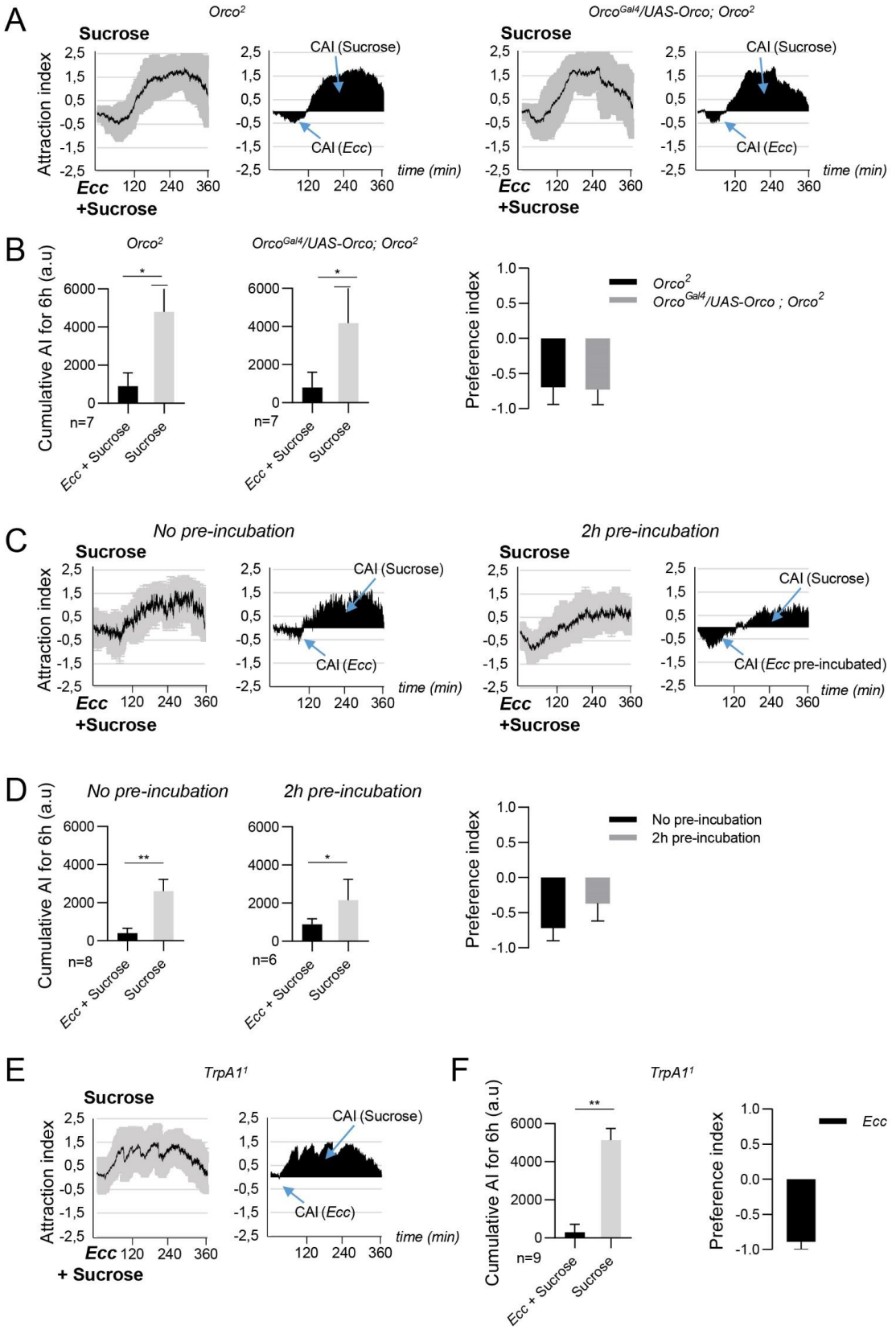

Figure S2. The odorant co-receptor Orco and the cation channel TrpA1 are not required for adult female's behavior to *Ecc*. Related to Figure 2.

A-B, *Orco*^{2} mutants and *Orco*^{2} rescued mutant (*Orco*^{Gal4}*/UAS-Orco; Orco*^{2}) displayed a two-step behavior. A, (Left graphs) Kinetic of the AI for sucrose in a sucrose versus sucrose + *Ecc* experiment. (Right graphs) CAI area for each specified solution (arrows) and its distribution over time. B, Histograms built with the CAI values from A. * P value< 0,05. Wilcoxon matched-pairs signed-rank test, Two-tailed P value. Error bars correspond to standard deviation. The preference indexes for *Ecc* are calculated with the CAI values from B. C-D, Pre-incubation of *Ecc* with sucrose does not affect the two-step behavior of adult females. C, (Left graphs) Kinetic of the AI for sucrose when flies were given the choice between an *Ecc* contaminated sucrose solution versus sucrose only or an *Ecc* contaminated sucrose solution pre-incubated 2h without flies versus sucrose only. (Right graphs) CAI area for each specified solution (arrows) and its distribution over time. D, Histograms built with the CAI values from C. * P value< 0,05 and ** P value< 0,01. Wilcoxon matched-pairs signed rank test, Two-tailed P value. Error bars correspond to standard deviation. The preference indexes for *Ecc* are calculated with the CAI values from D. E-F, Flies homozygotes for the loss of function allele *TrpA1*^{1} display aversion to *Ecc*. E, (Left graph) Kinetic of the AI index for Sucrose. (Right graph) CAI area for each specified solution (arrows) and its distribution over time. F, Histograms built with the CAI values from E. ** P value< 0,01. Wilcoxon matched-pairs signed rank test, Two-tailed P value. Error bars correspond to standard deviation. The preference index for *Ecc* calculated with the CAI values from F. For A, C and E left graphs, the black lines and the grey lines correspond respectively to the mean and the standard deviation, and for right graphs sole the mean value of the CAI obtained with multiple replicates is shown in black. n indicates the number of experimental replicates. a.u: arbitrary unit. Data are represented as mean +/- SD.

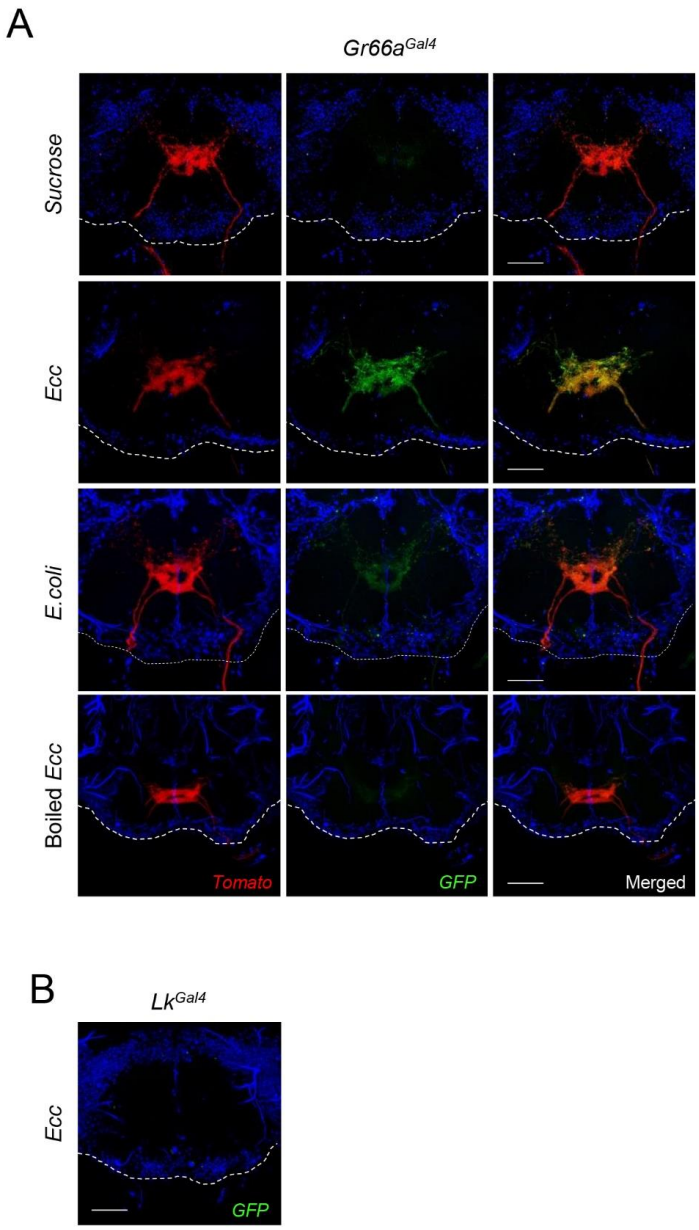

Figure S3. *Ecc* activates Ca^{+} release in *Gr66a* positive neurons but not in *Lk* positive ones. Related to Figure 5.

A, *Ecc*, and to a less extend *E. coli,* activates Ca^{+} release in Gr66a bitter neurons, but sucrose or boiled *Ecc* do not. Confocal images of the SEZ region of adult fly's brain of genotype *LexAop-CD8-GFP-2A-CD8-GFP; UAS-mLexA-VP16-NFAT/UAS-CD4::Tomato, lexAop-rCD2-GFP/Gr66a^{Gal4}*, that were fed with either Sucrose, *Ecc* + sucrose or *E.coli* + sucrose solutions. B, *Ecc* does not activates Ca^{+} release in Lk neurons. Confocal images of the SEZ region of adult fly's brain of genotype *LexAop-CD8-GFP-2A-CD8-GFP; UAS-mLexA-VP16-NFAT/UAS-CD4::Tomato, lexAop-rCD2-GFP/Lk^{Gal4}*, that were fed with either *Ecc* + sucrose solutions. For A and B, Red: Tomato, Green: GFP and Blue: nuclei staining with Hoechst. The dashed line is demarcating the brain periphery. Scale bar: 25 μm.

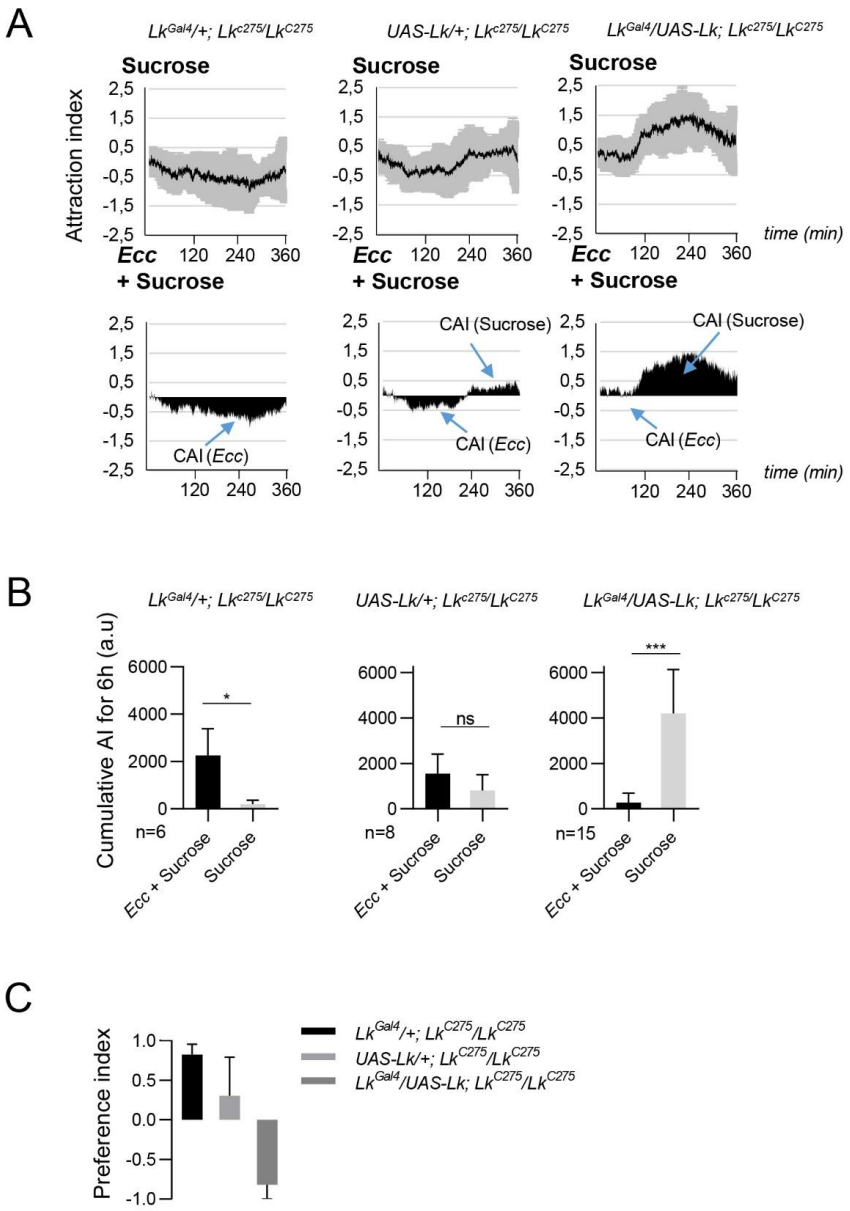

Figure S4. The neuropeptide Lk is required for the aversive perception of *Ecc.* Related to Figure 6.

A-B, Expression of *UAS-Lk* under the control of Lk^{Gal4} rescue the abnormal behavior observed for Lk^{c275} mutants. A, (Up) Kinetic of the AI for Sucrose. (Bottom) CAI area for each specified solution (arrows) and its distribution over time. B, Histograms built with the CAI values from A. * P value< 0,05 and *** P value< 0,001. ns, not significant. Wilcoxon matched-pairs signed rank test, Two-tailed P value. Error bars correspond to standard deviation. C, preference index for *Ecc* calculated with the CAI from B. A (top) the black lines and the grey lines correspond respectively to the mean and the standard deviation, and for bottom graphs, sole the mean value of the CAI obtained with multiple replicates is shown in black. n indicates the number of experimental replicates. a.u: arbitrary unit. Data are represented as mean +/- SD.

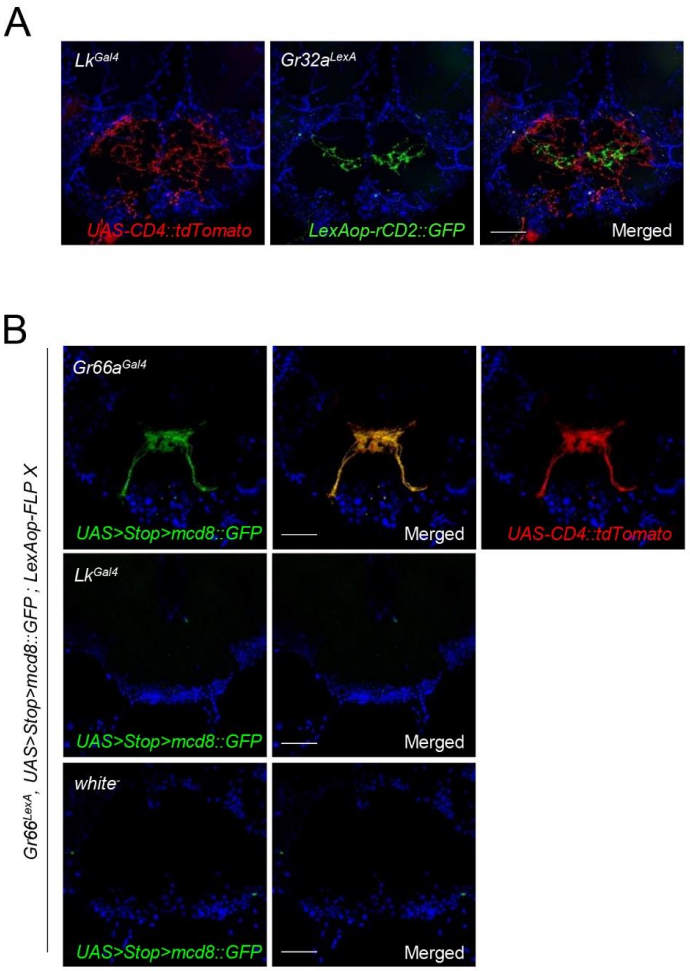

Figure S5. SEZ projections of Lk and bitter neurons are distinct. **Related to Figure 6.**

Confocal images of the SEZ region of adult brains showing that *Lk^{Gal4}* projections (red) do not co-localize with bitter neuron projections labelled with *Gr32^{LexA}* (green). Fly genotype is *Lk^{Gal4}/UAS-CD4::tdTomato ; Gr32^{LexA}/LexAop-rCD2::GFP*. B, leukokinin positive neurons do not share common identity with *Gr66^{LexA}* positive ones in the SEZ. Confocal images of the SEZ region of adult brains allowing activation of *UAS-mcd8::GFP* exclusively in Gr*66^{LexA}* positive cells (*Gr66^{LexA}, UAS>Stop>mcd8::GFP ; LexAop FLP*). As expected, crossing these flies to *Gr66^{Gal4}; UAS-CD4::tdTomato* flies, lead to *UAS-mcd8::GFP* expression in the SEZ (green) that perfectly match the expression of *UAS-CD4::tdTomato* (Red). No GFP positive cells are detectable using either *Lk^{Gal4}* or the control *white$^-$* fly strain. Blue: nuclei staining with Hoechst. Scale bar: 25 μm.

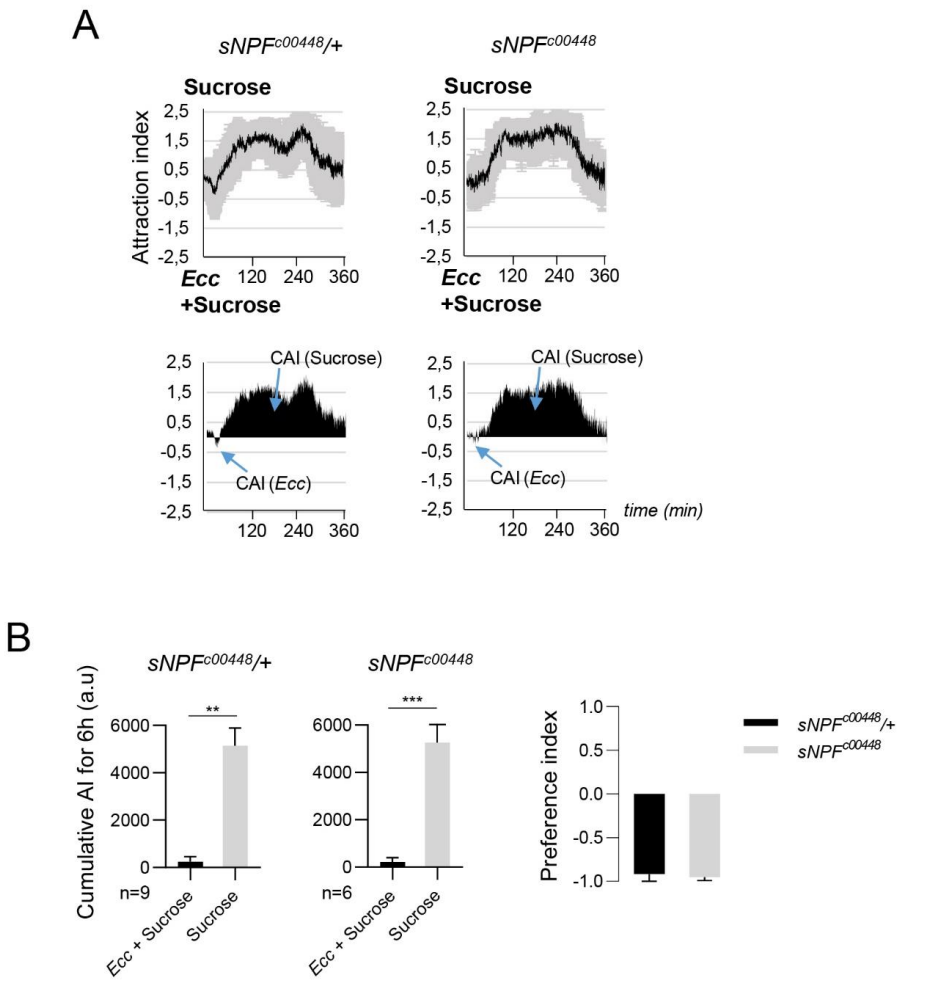

Figure S6. The short neuropeptide F is not required for the two-step behavior toward *Ecc.* Related to Figure 2.

A-B, *sNPF*^{c00488} mutants females displayed a normal two-step behavior as control *sNPF*^{c00488}/+ ones. A, (Top graphs) Kinetic of the AI for sucrose in a sucrose versus sucrose + *Ecc* experiment. (Bottom graphs) CAI area for each specified solution (arrows) and its distribution over time. B, Histograms built with the CAI values from A. ** P value< 0,01 and *** P value< 0,001. Wilcoxon matched-pairs signed-rank test, Two-tailed P value. Error bars correspond to standard deviation. The preference indexes for *Ecc* are calculated with the CAI values from B. For A top graphs, the black lines and the grey lines correspond respectively to the mean and the standard deviation, and for bottom graphs sole the mean value of the CAI obtained with multiple replicates is shown in black. n indicates the number of experimental replicates. a.u: arbitrary unit. Data are represented as mean +/- SD.

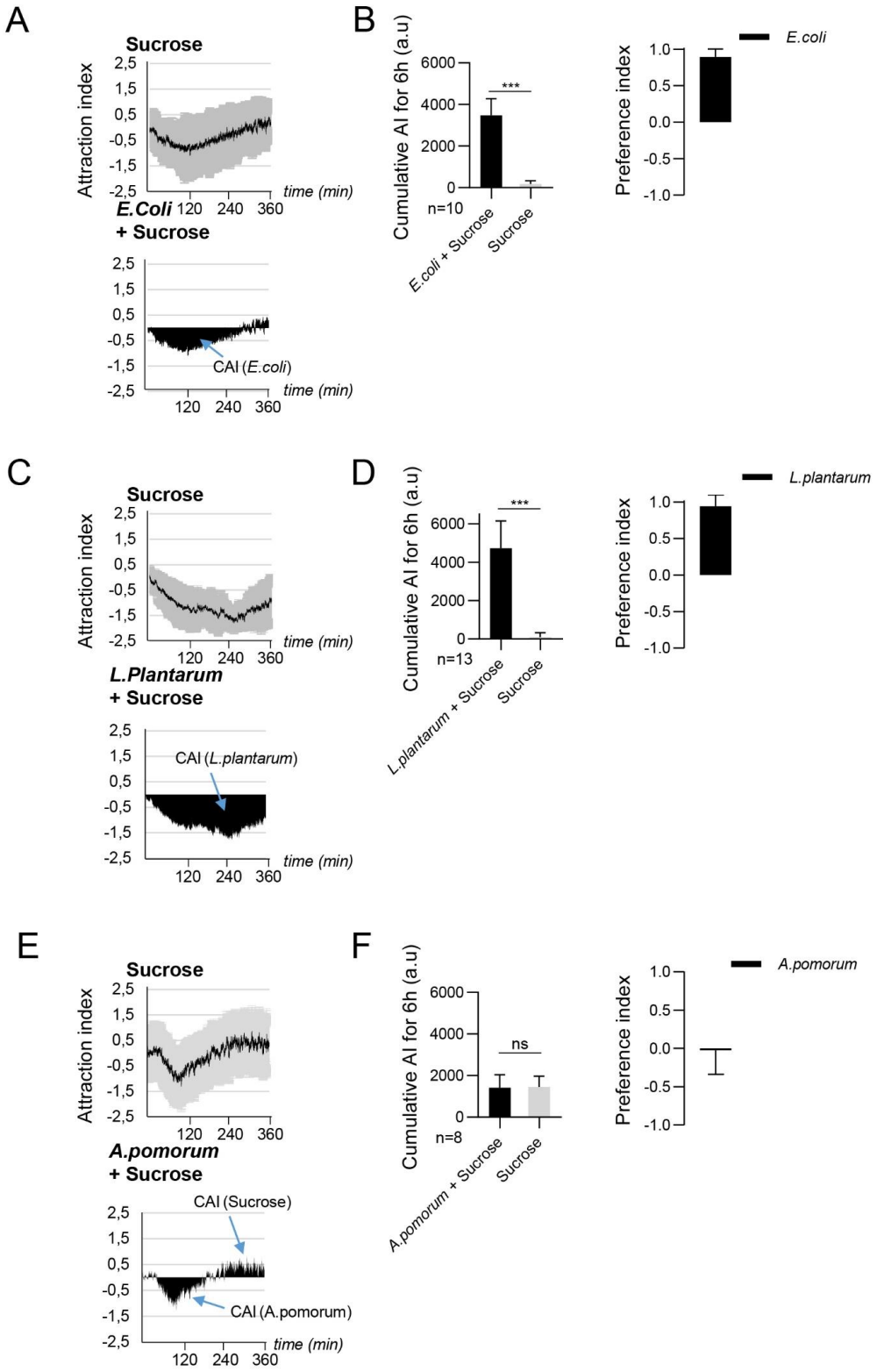

Figure S7. *D. melanogaster* adults display no aversion to either *E. coli*, *L. plantarum* or *A. pomorum* contaminated solutions. Related to Figure 2.

For A, C and E, the upper graphs show the kinetic of the AI for sucrose and the bottom graphs illustrate the CAI area for each solutions (arrows) and its distribution over time. For B, D and F, (left) graphs

correspond to histograms built with the CAI values from A, C and E, respectively. Right graphs are preference index for the bacteria contaminated solution calculated with the CAI values from B, D and F, respectively. A-B, Flies have a strong and statistically significant preference for sucrose + *E. coli* versus Sucrose. *** P value< 0,001. Wilcoxon matched-pairs signed rank test, Two-tailed P value. Error bars correspond to standard deviation. C-D, Flies had a strong and statistically significant preference for sucrose + *L. plantarum* versus Sucrose. *** P value< 0,001. Wilcoxon matched-pairs signed rank test, Two-tailed P value. Error bars correspond to standard deviation. E-F, flies had no preference for sucrose + *A.pomorum* versus Sucrose. ns, not significant. Wilcoxon matched-pairs signed rank test, Two-tailed P value. Error bars correspond to standard deviation. For A, C and E (top): the black lines and the grey lines correspond respectively to the mean and the standard deviation, and for bottom graphs, sole the mean value of the CAI obtained with multiple replicates is shown in black. n indicates the number of experimental replicates. a.u: arbitrary unit. Data are represented as mean +/- SD.

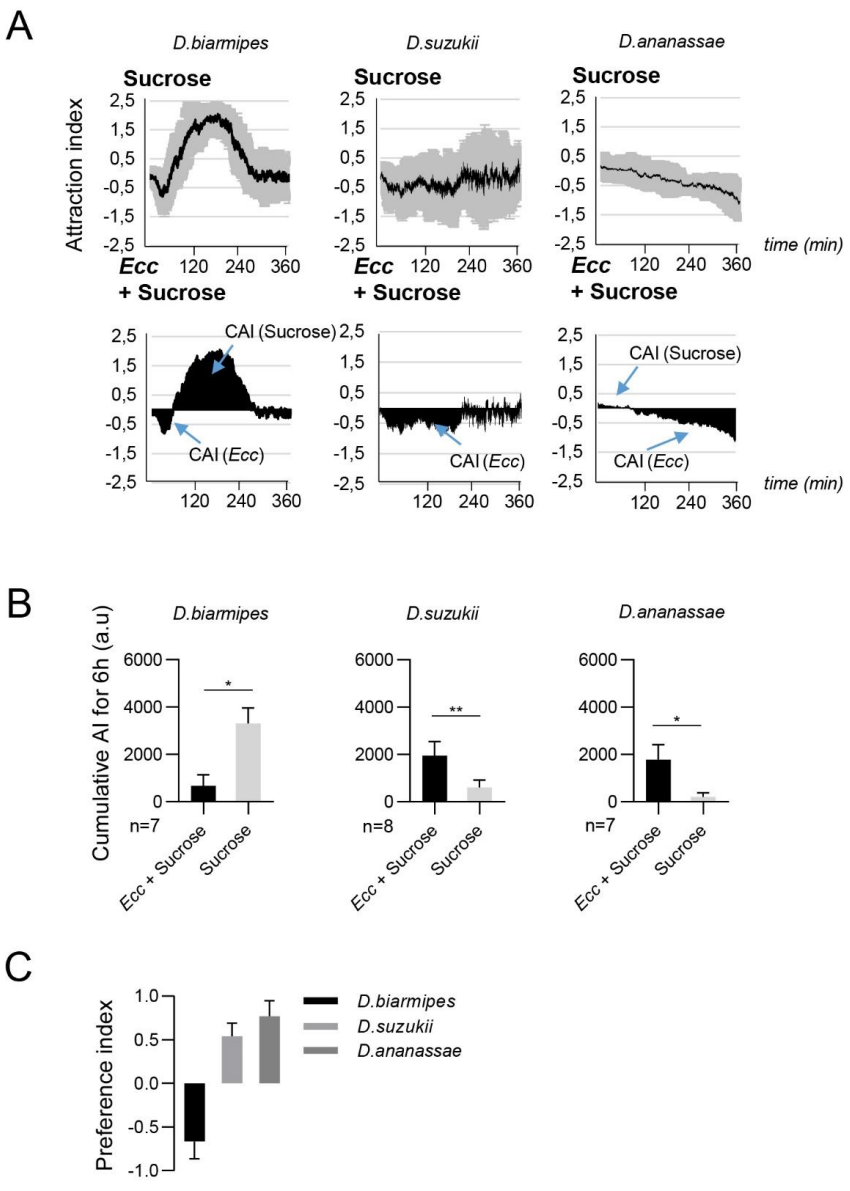

Figure S8. *D. melanogaster* behavior towards *Ecc* is species-specific. Related to Figure 2.

A, (Up) Kinetic of the AI index for Sucrose. (Down) CAI area for each specified solution (arrows) and its distribution over time. B, Histograms built with the CAI values from A. *D. biarmipes* have a strong and statistically significant preference for sucrose versus sucrose + *Ecc* while *D. suzukii* and *D. ananassae* prefer the contaminated solution versus Sucrose. * P value< 0,05 and ** P value< 0,01. Wilcoxon matched-pairs signed rank test, Two-tailed P value. Error bars correspond to standard deviation. C, preference index for *Ecc* calculated with the CAI values from B. A (top) the black lines and the grey lines correspond respectively to the mean and the standard deviation, and for bottom graphs, sole the mean value of the CAI obtained with multiple replicates is shown in black. n indicates the number of experimental replicates. a.u: arbitrary unit. Data are represented as mean +/- SD.

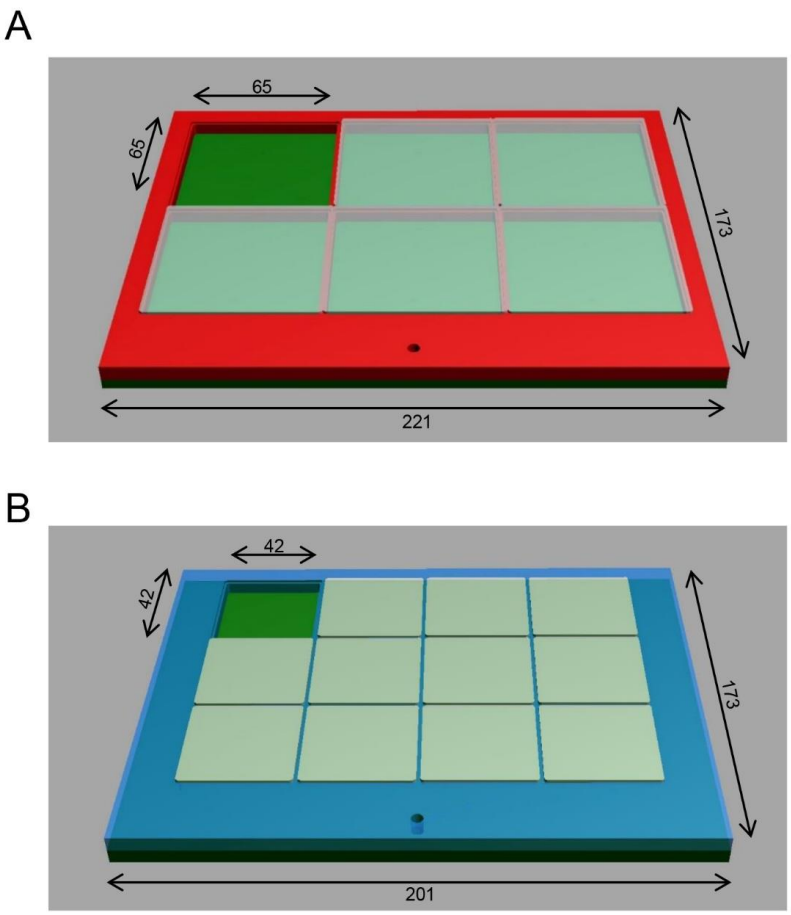

Figure S9. Dimensions of the apparatus used for behavioral assays. Related to STAR Methods.

A-B, Cartoon of the 6 arenas and the 12 arenas apparatus with the dimensions indicated in millimeters. Each apparatus is composed of three distinct plastic parts, the bottom part (dark green) which is a flat plain slab on top of which is glued the plastic grid containing 6 (red in A) or 12 (blue in B) squared holes and the 6 (or 12) removable plastic caps (light green in A and B) used to cover the arenas. The holes shown in A and B is used to screw the plastic arm (not shown here) design to fix the camera on top of the apparatus.

Transparent Methods

D.melanogaster strains and maintenance

The strains used in this work are: w^{1118} BL#3605, *CantonS* BL#64349, $orco^{2}$ BL#23130, $Orco^{Gal4}$ (Larsson et al., 2004), *UAS-Orco* BL#23145, $Relish^{E20}$ (Hedengren et al., 1999), *Df(3R)ED5301* BL#9225, $Gr66a^{Gal4}$ BL#57670, *UAS-Kir2.1::EGFP* BL#6595, $Gr66a^{ex83}$ BL#25027, $Gr66a^{+t8}$; $Gr66a^{ex83}$ BL#35528, $Gr33a^{1}$ BL#31425, *Tl*{*Gal4*}$Gr33a^{Gal4}$ BL#31427, $Gr33a^{1}$; UAS-*Gr33a* BL#31424, Lk^{C275} BL#16324, $G\alpha q^{1}$ BL#42257, $TrpA1^{1}$ BL#26504, *UAS-CD4::tdTomato* BL#35841, *UAS-CaLexA* BL#66542, Lk^{Gal4} BL#51993, *UAS>Stop>mcd8::GFP* BL#30125, $Gr66a^{LexA}$ (from Kristin Scott), $Gr32a^{LexA}$ (from Anupama Arun Dahanukar), *LexAop-FLP* BL#55819, *LexAop-rCD2::GFP* BL#66544, *UAS-Lk* (this work, molecular detail of the construct under request) $Diptericin\text{-}Cherry^{C1}$ (Charroux and Royet, 2009), $PGRP\text{-}LB^{\Delta}$ (Paredes et al., 2011), $Gr5a^{Gal4}$ BL#57591, $R1Gr5a^{LexA}$;; $\Delta Gr61a,\Delta Gr64a\text{-}f$ and $Gr43a^{-}$ (*Tl{GAL4}*$Gr43a^{GAL4}$) (from Hubert Amrein), $Gr63a^{1}$ BL#9941, $UAS\text{-}Oct\text{-}TyrR^{RNAi}$ BL# 28332 and $sNPF^{c00448}$ (from Michael D. Gordon). Flies were grown at 25°C on a yeast/cornmeal medium in 12h/12h light/dark cycle-controlled incubators. For 1liter of food, 8.2g of agar (VWR, cat. #20768.361), 80g of cornmeal flour (Westhove, Farigel maize H1) and 80g of yeast extract (VWR, cat. #24979.413) were cooked for 10 min in boiling water. 5.2 g of Methylparaben sodium salt (MERCK, cat. #106756) and 4 ml of 99% propionic acid (CARLOERBA, cat. #409553) were added when the food had cooled down. For antibiotic (ATB) treatment, the standard medium was supplemented with Ampicillin, Kanamycin, Tetracyclin and, Erythromycin at 50 µg/ml final concentrations.

Imaging

Adult tissues were dissected in PBS, fixed for 20 min in 4% paraformaldehyde on ice and rinsed 3 times in PBT (PBS + 0.1% Triton X-100). The tissues were mounted in Vectashield (Vector Laboratories) fluorescent mounting medium, with or without DAPI. Images were captured with an LSM 780 Zeiss confocal microscope.

Bacterial strains

The following microorganisms were used: *Erwinia carotovora carotovora 15* 2141 (grown at 30°C), *Erwinia carotovora carotovora 15 pOM1-GFP* (grown at 30°C), $Lactobacillus\ plantarum^{WJL}$ (grown at 37°C), *Escherichia coli* strain DH5 α (grown at 37°C) and *Acetobacter pomorum* (grown at 30°C). Bacteria were cultured overnight in Luria-Bertani (for *Ecc*, *Ecc-GFP* and *E. coli*) or MRS medium (for *L.plantarum* and *A. pomorum*). Bacterial cultures were centrifuged at 4000 g for 15 min at RT and re-suspended in 1XPBS. Cells were serially diluted in PBS and their concentration was determined by optical density (OD) measurement at 600 nm.

Fly preparation and chemical used in behavioral assays

We used 4-6 days old flies raised at 25°C in presence of ATB in the food. Flies were starved during 16h before the behavioral assay using empty vial with no food closed by a plug soaked with 500 µl of water. 10 to 20 flies were anesthetized on the ice for 5 minutes and loaded in each arena of our apparatus, where two drops of a given solution were previously deposited. We used the following compound from Sigma-Aldrich: sucrose (cat #S1888), caffeine (cat #C0750) and Eriauglaucine blue (Sigma-Aldrich, cat #861146) at 125 µg/ml final concentration to color the liquid solutions. All behavioral experiments using bacteria were performed with bacteria diluted at OD_{600}=50 in 50 mM sucrose (excepted for Figure 7E where a serial dilution of *Ecc* in 50 mM sucrose was used). For *Ecc* heat inactivation, a solution of *Ecc* diluted in 50 mM sucrose (final OD_{600}=50) was incubated at 96°C for 20 minutes, then cool down before use. All experiments were performed in a behavioral room with constant temperature (24°C) and humidity (65%). The dimensions of the apparatus used for behavioral assays (the 6 arenas and the 12 arenas apparatus) are shown in Figures S9A-B.

Bacterial Load Analysis

Bacterial load of surface-sterilized individuals was quantified by plating serial dilutions of lysates obtained from a single individual on a nutrient agar plate. Biological triplicates were collected for each experimental condition. Homogenization of individuals or tissues was performed using the Precellys 24 tissue homogenizer (Bertin Technologies, France) and 0.75/1 mm glass beads in 800 ml of the appropriate bacterial culture medium.

Adult oral infection

We used 4-6 days old female raised at 25°C in presence of ATB in the food. 24h before the infection, female flies were transferred in vials without ATB and then placed in a fly vial with *Ecc* contaminated food. The food solution was obtained by mixing a pellet of an overnight culture of bacteria *Ecc-15* (OD=200) with a solution of 5% sucrose (50/50) and added to a filter disk that completely covered the agar surface of the fly vial. Flies were incubated at 25°C for 24h.

Statistical Analysis

The Prism software (GraphPad) was used for statistical analyses. We used the nonparametric Wilcoxon matched-pairs signed-rank test. P value was indicated as follow: * for P<0,05, ** for P<0,01, *** for P<0,001. ns for not significantly different.

Flybox

For video/frame processing and analysis, we have developed a homemade software called *Flybox* which can track up to six different experiment boxes simultaneously. Video/frame processing and analysis have been achieved using MATLAB R2015B, Statistical Toolbox and, Image Analysis Toolbox.

Given a movie M:

$$M = (F_0, ..., F_n)$$

where n denotes the number of frames into M, every frames of M are composed of three-color components (RGB)

$$F_k = (R_k, G_k, B_k) \in M$$

where k stands for the kth frame into the movie M

Droplet solution detection and localization

As the size and shape of the two droplet solutions per box were possibly evolving throughout the whole movie depending on fly appetite, we decided to take only the first video frame as a reference for the subsequent droplet solution detection and localization analysis and a user input feedback to assign a qualitative label to every droplet solution content. As a preprocessing step, we converted the original frame color space from RGB to HSV (Hue Saturation Value) to keep only the saturation as the color intensity of the two droplets was different from the background into this component. We used a bit depth value *b* of 255 (8-bits) to rescale pixel values to be in the 0-1 range.

$$F_0' = \frac{F_0}{b}$$

We calculated the saturation component of the reference frame as:

$$S = \begin{cases} 0 & \text{if} \quad max(F_0') = 0 \\ 1 - \frac{min(F_0')}{max(F_0')} & \text{otherwise} \end{cases}$$

We binarized this image to create the droplet masks by using a binarization threshold value α to 0,5.

$$B_{droplets} = \begin{cases} 0 & \text{if} \quad S < \alpha \\ 1 & \text{otherwise} \end{cases}$$

To extract droplets from this binary mask, we extracted all 8-connected components, and we discarded those having less than 50 pixels as total area to avoid false positive detections and keeping only the two true positive droplets into two individual masks D1 and D2:

$$(D_1, D_2) = ConnComp(B_{droplets})$$

We then extracted droplet centroids:

$$c_{D_k} = \left(\frac{1}{n} \sum_{i=1}^{n} x_i \quad ; \frac{1}{n} \sum_{i=1}^{n} y_i \right) ; (x_i, y_i) \in D_k$$

and we assigned them their corresponding user-defined label.

Fly detection and localization

The fly detection process is achieved for each video frame independently and into every experimental box simultaneously. Starting from the original RGB image, we subtracted the red from the green component to be able to decrease the blueish color of the droplet solution without altering the fly original blackish colors.

$$H_k = G_k - R_k$$

We then applied a Gaussian smoothing filter using σ =2 to both hide small image artifacts and unsharp fly bodies to help in their further detection.

$$Gauss_k = \frac{1}{2\pi\sigma^2} e^{\frac{-(x^2+y^2)}{2\sigma^2}}; (x,y) \in H_k$$

We noticed that pixels coming from the background are both overrepresented and have a rather uniform pixel intensity which is not the case of pixels coming from fly bodies which are underrepresented. To easily discriminates the two sets of pixels, we decided to rescale every pixel intensity using a z-score scaling procedure by keeping only ones having a large standard deviation (z-score>11).

$$B_{flies} = \begin{cases} 0 & \text{if} \quad \frac{Gauss_k - \mu(Gauss_k)}{\sigma(Gauss_k)} < 11 \\ 1 & \text{otherwise} \end{cases}$$

We extracted all 8-connected components as individual flies:

$$(Fly_1, ..., Fly_m) = ConnComp(B_{flies})$$

and we calculated centroid coordinates for every detected fly:

$$c_{Fly_k} = \left(\frac{1}{n} \sum_{i=1}^{n} x_i \quad ; \frac{1}{n} \sum_{i=1}^{n} y_i \right); (x_i, y_i) \in Fly_k$$

Quantifying the droplet solution preference for the overall fly populationWe started from the hypothesis that a population of fly attracted by one particular droplet solution should spend more time close to it relative to the other one. First, we calculated an *attraction index* as the log2 ratio of the sum of Euclidean distance of flies to each droplet:

$$attractivity(F_k) = log_2 \left(\frac{\sum_{k=1}^{m} \| c_{D1} - c_{Fly_k} \|}{\sum_{k=1}^{m} \| c_{D_2} - c_{Fly_k} \|} \right)$$

As a result, for a given frame, we can measure the overall attraction of one particular droplet solution relative to the other: D2 attraction will be translated into a positive index value and D1 by a negative. The strength of attraction can also be assessed as the absolute difference between the index value and zero value: high index values (positive or negative) are then correlated with high attraction (resp. low index for low attraction) Then, for every droplet, D1 and D2, we independently calculated a *Cumulative Attraction Index* (CAI) as the total area under the curve of either each negative or each positive

attraction *indexes* throughout the whole movie. To differentiate the two cases (negative and positive attraction indexes), we first defined two logical functions *pos* and *neg* as:

$$pos(F_k) = \begin{cases} 1 & \text{if} \quad attractivity(F_k) > 0 \\ 0 & \text{otherwise} \end{cases}$$

$$neg(F_k) = \begin{cases} 1 & \text{if} \quad attractivity(F_k) < 0 \\ 0 & \text{otherwise} \end{cases}$$

and finally, *the preference index* (named CAI in the main text) as the trapezoidal numerical integration of attraction indexes calculated throughout the whole movie:

$$preferenceD_2(M) \approx \frac{1}{2n} \sum_{i=1}^{n} (pos(F_i - 1) \cdot attractivity(F_i - 1) + pos(F_i) \cdot attractivity(F_i))$$

Supplemental References

Larsson, M.C., Domingos, A.I., Jones, W.D., Chiappe, M.E., Amrein, H., and Vosshall, L.B. (2004). Or83b encodes a broadly expressed odorant receptor essential for Drosophila olfaction. Neuron *43*, 703-714.

Hedengren, M., Asling, B., Dushay, M.S., Ando, I., Ekengren, S., Wihlborg, M., and Hultmark, D. (1999).

Charroux, B., and Royet, J. (2009). Elimination of plasmatocytes by targeted apoptosis reveals their role in multiple aspects of the Drosophila immune response. Proc Natl Acad Sci U S A *106*, 9797-9802.

Paredes, J.C., Welchman, D.P., Poidevin, M., and Lemaitre, B. (2011). Negative regulation by amidase PGRPs shapes the Drosophila antibacterial response and protects the fly from innocuous infection. Immunity *35*, 770-779.